

Phase transitions and light scalars in bottom-up holography

Daniel Elander¹, Ali Fatemiabhari^{2,*} and Maurizio Piai²

¹*Laboratoire Charles Coulomb (L2C), University of Montpellier, CNRS, Place Eugène Bataillon - CC069, F-34095 Montpellier Cedex 5, France*

²*Department of Physics, Faculty of Science and Engineering, Swansea University, Singleton Park, SA2 8PP, Swansea, Wales, United Kingdom*



(Received 11 January 2023; accepted 19 June 2023; published 19 July 2023)

Within the bottom-up approach to holography, we construct a class of six-dimensional gravity models and discuss solutions that can be interpreted, asymptotically in the far UV, in terms of dual five-dimensional conformal field theories deformed by a single scalar operator. We treat the scaling dimension of this operator, related to the mass of the one scalar field in the gravity theory, as a free parameter. One dimension in the regular geometry is compactified on a shrinking circle, hence mimicking confinement in the resulting dual four-dimensional theories. We study the mass spectrum of bosonic states. The lightest state in this spectrum is a scalar particle. Along the regular (confining) branch of solutions, we find the presence of a tachyonic instability in part of the parameter space, reached by a smooth deformation of the mass spectrum, as a function of the boundary value of the background scalar field in the gravity theory. In a region of parameter space nearby the tachyonic one, the lightest scalar particle can be interpreted as an approximate dilaton, sourced by the trace of the stress-energy tensor, and its mass is parametrically suppressed. We also compute the free energy, along several branches of gravity solutions. We find that both the dilatonic and tachyonic regions of parameter space, identified along the branch of confining solutions, are hidden behind a first-order phase transition, so that they are not realized as stable solutions, irrespectively of the scaling dimension of the deforming field-theory operator. The (approximate) dilaton, in particular, appears in metastable solutions. Yet, the mass of the lightest state, computed close to the phase transition, is (mildly) suppressed. This feature is amplified when the (free) parameter controlling the scaling dimension of the deformation is $5/2$, half the dimension of space-time in the field theory.

DOI: [10.1103/PhysRevD.108.015021](https://doi.org/10.1103/PhysRevD.108.015021)

I. INTRODUCTION

Investigations into the fundamental nature and origin of the Higgs boson, the latest particle of the Standard Model (SM) to have been discovered [1,2], are among the most topical in theoretical physics, in view of the ongoing precision experimental program at the Large Hadron Collider. Because of the approximate (explicitly and spontaneously broken) scale-invariant nature of the SM theory, the Higgs boson itself is in fact a dilaton, the pseudo-Nambu-Goldstone boson associated with dilatations. It is natural to question whether this is just an accidental symmetry in the SM, or whether it has a more fundamental, important origin and role [3]. In particular, is it possible for the Higgs boson to originate as a composite

dilaton in a more fundamental theory? And if so, what type of underlying dynamics would yield realistic values for its mass and couplings?

The literature on the dilaton effective field theory dates back many decades [4,5], and its applications have been long discussed in the context of dynamical electroweak symmetry breaking [6–8], extensions of the SM [9–19], and, more recently, the interpretation of lattice data [20–36], in particular in view of the numerical work on certain $SU(3)$ gauge theories that show indications of a light scalar bound state in the spectrum [37–48].

The context of gauge-gravity dualities [49–52] is particularly suitable for describing the dilaton and its dynamical origin, both in its bottom-up [53–67] as well as top-down [68–72] realizations. In what follows, we restrict our attention to holographic duals in which the geometry of a completely smooth classical background in a higher-dimensional gravity theory contains a shrinking circle, the shrinking of which can be used to mimic confinement in the dual field theory, as suggested in Ref. [73]—see also Refs. [74–80]. The spectra of bound states of the strongly coupled theory can be computed perturbatively in its gravity dual, by

*a.fatemiabhari.2127756@swansea.ac.uk

Published by the American Physical Society under the terms of the [Creative Commons Attribution 4.0 International license](https://creativecommons.org/licenses/by/4.0/). Further distribution of this work must maintain attribution to the author(s) and the published article's title, journal citation, and DOI. Funded by SCOAP³.

exploiting the holographic gauge-invariant formalism developed in Refs. [81–85]—see also Refs. [70–72,80,86]. A useful diagnostic tool to identify (approximate) dilatons within such spectra is provided by the probe approximation, as discussed in Ref. [86]. Furthermore, one can apply holographic renormalization [87–89] to compute field-theory quantities, such as the free energy. We also find it appealing to adopt a simple scale-setting procedure, such as that proposed in Ref. [90].

Among all possible realizations of the dilaton scenario, we concentrate on the ideas developed in Refs. [91–94]—see also Ref. [95] and references therein. Namely, we want to understand whether a light dilaton state might arise in strongly coupled theories, the renormalization group (RG) flow of which brings them in close proximity of a tachyonic instability. In the holographic dual description of conformal field theories (CFTs)—fixed points of the RG flow—the notion of the Breitenlohner-Freedman bound [96] captures the type of instability of interest. In the case of confining theories, one can generalize this notion and ultimately arrive to the following, similar conclusions for physical observables [97–99]. In summary, the classical instability is resolved by the presence of a first-order phase transition. The unstable region of parameter space cannot be physically realized, which protects the physical spectrum from developing a tachyon. Nevertheless, one may ask whether, for choices of parameters close to the phase transition, the lightest (neutral) scalar in the spectrum has mass and properties that are influenced by the presence of the tachyonic instability itself, even if the latter is only present in an unphysical region of parameter space.

The analysis of Refs. [97–99] indicates that it is possible to realize this scenario within well-established examples of top-down holographic models, derived as classical solutions of supergravities in various dimensions. In all three cases analyzed so far, it has been found that for choices of the parameters that are close to the phase transition boundary, the lightest scalar state is not parametrically light, as was predicted in Ref. [94], on the basis of the results from a bottom-up model obtained in a dedicated construction—for models in which no light dilaton is present, see for instance Refs. [100,101].

In this paper, inspired by Refs. [97–99], we build a class of bottom-up models that combine the quadratic superpotential adopted in Ref. [54] and the confinement mechanism in Ref. [73]. We assume that the holographic description of the dynamics be encapsulated in a model consisting of one real scalar, coupled to gravity in $D = 6$ dimensions, one of which is compactified on a circle. Along the interesting, physical branch of solutions the circle shrinks to a point at a finite position along the holographic dimension, introducing a dynamical scale, but the geometry is regular and smooth everywhere. What results is the dual description of a putative family of four-dimensional, confining theories, that at short distances are best described by the circle compactification of a five-dimensional CFT in the presence of an operator with

nontrivial dimension given by $\max(\Delta, 5 - \Delta)$, where Δ is a free parameter appearing in the scalar potential of the gravity theory.

The generic behavior of the model, for each value of Δ , is qualitatively similar to that found in Refs. [97–99] and described above, as we shall show. The advantage of the bottom-up approach—aside from having a much simpler bosonic action—is that it allows us to vary Δ . We are interested in the relation between Δ and the mass spectrum, in particular for the lightest scalar, and in proximity of the phase transition.

The paper is organized as follows. We start by defining the gravity theory in $D = 6$ dimensions, in Sec. II. We present several classes of classical solutions in Sec. III and then study the spectrum of small fluctuations for one of these classes, the regular (confining) branch of solutions, in Sec. IV. The free energy of the different classes of solutions is discussed in Sec. V, where we analyze which branch of solutions is energetically favored, depending on the parameters of the model. We summarize the most salient numerical results in Sec. VI and outline future lines of research in Sec. VII, while relegating to the Appendixes many useful technical details.

II. THE MODEL

This section introduces a model, built within the context of bottom-up holography, that describes a real scalar field ϕ coupled to gravity in $D = 6$ dimensions, with a simple quartic scalar potential [54]. The scalar field captures, in the gravity language, the effects of the deformation of the dual five-dimensional CFT by a scalar operator, as well as the formation of the corresponding condensate. Furthermore, one of the dimensions is compactified on a circle (in both field theory as well as gravity). As we shall see in Sec. III, this system admits solutions in which the circle shrinks smoothly at the end of space in the IR, thus introducing a physical low-energy scale, while mimicking (in analogy with top-down models) the effect of confinement in what would be the dual, four-dimensional field theory [73]. We also find it convenient to provide the description of the gravity theory in $D = 5$ dimensions, obtained after reduction on the circle.

A. Action in six dimensions

We follow the conventions in Ref. [86] (see also references therein), which we summarize in Appendix A. In order for the model to mimic the dual of a four-dimensional confining theory, we choose to work in $D = 6$ dimensions. The action is the following:

$$\mathcal{S}_6 = \mathcal{S}_6^{(\text{bulk})} + \sum_{i=1,2} \mathcal{S}_{5,i}, \quad (1)$$

$$\mathcal{S}_6^{(\text{bulk})} = \int d^6x \sqrt{-\hat{g}_6} \left\{ \frac{\mathcal{R}_6}{4} - \frac{1}{2} \hat{g}^{\hat{M}\hat{N}} \partial_{\hat{M}} \phi \partial_{\hat{N}} \phi - V_6(\phi) \right\}, \quad (2)$$

$$\mathcal{S}_{5,i} = (-)^i \int d^5x \sqrt{-\tilde{g}} \left\{ \frac{\mathcal{K}}{2} + \lambda_i(\phi) + f_i(\tilde{g}_{\hat{M}\hat{N}}) \right\} \Big|_{\rho=\rho_i}, \quad (3)$$

and besides the bulk part, $\mathcal{S}_6^{(\text{bulk})}$, it contains also two boundary actions, $\mathcal{S}_{5,i}$, localized at the boundaries of the radial coordinate $\rho_1 < \rho < \rho_2$. The space-time index is $\hat{M} = 0, 1, 2, 3, 5, 6$. The extrinsic curvature \mathcal{K} , appearing in the Gibbons-Hawking-York term of the boundary actions, depends on the induced metric on the boundaries, denoted $\tilde{g}_{\hat{M}\hat{N}}$.

For the bulk potential \mathcal{V}_6 , we choose to write

$$\begin{aligned} \mathcal{V}_6(\phi) &= \frac{1}{2} \left(\frac{\partial \mathcal{W}_6(\phi)}{\partial \phi} \right)^2 - \frac{5}{4} \mathcal{W}_6(\phi)^2 \\ &= -5 - \frac{\Delta(5-\Delta)}{2} \phi^2 - \frac{5\Delta^2}{16} \phi^4, \end{aligned} \quad (4)$$

where the superpotential is given by [54]

$$\mathcal{W}_6(\phi) \equiv -2 - \frac{\Delta}{2} \phi^2. \quad (5)$$

The choice of a simple quadratic superpotential provides a neat field-theory interpretation for backgrounds in which ϕ is nonzero: asymptotically in the UV, the dual field theory flows toward a CFT in $D-1=5$ dimensions, deformed by the insertion of an operator \mathcal{O} with scaling dimension given by $\max(\Delta, 5-\Delta)$, and the two parameters appearing in the solution of the corresponding second-order classical equations correspond in field-theory terms to the coupling and condensate associated with \mathcal{O} .

We treat Δ as a free parameter—in top-down models, by contrast, its counterpart descends from first principles. In all three examples discussed in Refs. [97–99], the first-order equations involve choices of $\Delta > (D-1)/2$ (where D is equal to 6, 7, and 5, respectively, in those three models). Later in the paper, we will discuss the differences emerging for $0 < \Delta < (D-1)/2 = 5/2$. For the time being, it suffices to notice that the counterterm used for holographic renormalization coincides with \mathcal{W}_6 when $\Delta < 5/2$, while for $\Delta > 5/2$ one needs the associated superpotential

$$\begin{aligned} \bar{\mathcal{W}}_6 &= -2 - \frac{1}{2} (5-\Delta) \phi^2 - \frac{25(2\Delta-5)}{16(4\Delta-15)} \phi^4 \\ &\quad - \frac{125(2\Delta-5)(4\Delta^2-15\Delta+25)}{64(4\Delta-15)^2(6\Delta-25)} \phi^6 + \dots, \end{aligned} \quad (6)$$

which is only known perturbatively in ϕ yet also solves Eq. (4). In Appendix B, we show this superpotential expanded to higher orders. Pathological values of $\Delta = \frac{15}{4}, \frac{25}{6}, \dots$ appear at increasing orders in ϕ . In the following,

we will avoid using these special pathological values. Another special case is $\Delta = 5/2$, which requires a separate treatment, as we shall see.

The boundary terms in Eq. (3) play an important role in this paper. They determine the boundary conditions for the classical background solutions, via the consistency requirements on the variational principle. They are used in the calculation of the spectrum of fluctuations around such background solutions. And finally, they enter into the calculation of the free energy—but notice that this last calculation requires a modification of the UV-boundary terms, in which λ_2 (and f_2) must be replaced by the counterterms required for holographic renormalization.

B. Dimensional reduction to five dimensions

One of the dimensions is compact, the coordinate $0 \leq \eta < 2\pi$ describing a circle. In reducing the action to five dimensions, we write the metric as

$$ds_6^2 = e^{-2\chi} dx_5^2 + e^{6\chi} (d\eta + \chi_M dx^M)^2, \quad (7)$$

where the space-time index is $M = 0, 1, 2, 3, 5$. The reduced action then becomes

$$\mathcal{S}_5 = \mathcal{S}_5^{(\text{bulk})} + \sum_{i=1,2} \mathcal{S}_{4,i}, \quad (8)$$

$$\begin{aligned} \mathcal{S}_5^{(\text{bulk})} &= \int d^5x \sqrt{-g_5} \left\{ \frac{R}{4} - \frac{1}{2} g^{MN} [6\partial_M \chi \partial_N \chi + \partial_M \phi \partial_N \phi] \right. \\ &\quad \left. - e^{-2\chi} \mathcal{V}_6(|\phi|) - \frac{1}{16} e^{8\chi} g^{MP} g^{NQ} F_{MN}^{(\chi)} F_{PQ}^{(\chi)} \right\}, \end{aligned} \quad (9)$$

$$\mathcal{S}_{4,i} = (-)^i \int d^4x \sqrt{-\tilde{g}} \left\{ \frac{\mathcal{K}}{2} + e^{-\chi} \lambda_i(\phi) + e^{-\chi} f_i(\chi) \right\} \Big|_{\rho=\rho_i}, \quad (10)$$

where the five-dimensional metric g_{MN} has determinant g_5 , the induced metric on the boundaries is \tilde{g}_{MN} , the five-dimensional Ricci scalar is R , and K is the extrinsic curvature. The field strength for the vector χ_M is given by $F_{MN}^{(\chi)} = \partial_M \chi_N - \partial_N \chi_M$. The functions f_i of the six-dimensional theory depend explicitly on χ , as is required in order to obtain solutions that lift to geometries in six dimensions in which the circle shrinks smoothly.

The scalars $\Phi^a = \{\phi, \chi\}$ describe a sigma model coupled to gravity, the action of which is the same as in Eq. (A1) with $D=5$ and sigma-model metric $G_{ab} = \text{diag}(1, 6)$. We consider background solutions in which $\chi_M = 0$, while the metric g_{MN} , ϕ , and χ depend on the radial coordinate only. The metric in five dimensions takes the domain-wall (DW) form

$$ds_5^2 = dr^2 + e^{2A(r)} dx_{1,3}^2 = e^{2\chi(\rho)} d\rho^2 + e^{2A(\rho)} dx_{1,3}^2, \quad (11)$$

where we have adopted the convenient choice of radial coordinate $d\rho = e^{-\chi} dr$. The background fields satisfy the equations of motion

$$\partial_\rho^2 \phi + (4\partial_\rho A - \partial_\rho \chi) \partial_\rho \phi = \frac{\partial \mathcal{V}_6}{\partial \phi}, \quad (12)$$

$$\partial_\rho^2 \chi + (4\partial_\rho A - \partial_\rho \chi) \partial_\rho \chi = -\frac{\mathcal{V}_6}{3}, \quad (13)$$

$$3(\partial_\rho A)^2 - \frac{1}{2}(\partial_\rho \phi)^2 - 3(\partial_\rho \chi)^2 = -\mathcal{V}_6, \quad (14)$$

with boundary conditions given by

$$\begin{aligned} \left(\partial_\rho \phi - \frac{\partial \lambda_i}{\partial \phi} \right) \Big|_{\rho_i} &= 0, \\ \left(6\partial_\rho \chi + \lambda_i + f_i - \frac{\partial f_i}{\partial \chi} \right) \Big|_{\rho_i} &= 0, \\ \left(\frac{3}{2} \partial_\rho A + \lambda_i + f_i \right) \Big|_{\rho_i} &= 0. \end{aligned} \quad (15)$$

For vanishing $f_i = 0$, one obtains solutions that lift to domain walls in six dimensions.

The solutions satisfy the following equation:

$$0 = 12(\partial_\rho A)^2 + 3\partial_\rho^2 A - 3\partial_\rho \chi \partial_\rho A + 4\mathcal{V}_6, \quad (16)$$

which can be combined with Eq. (13) to yield the conservation law (see also Ref. [97])

$$\partial_\rho [e^{4A-\chi} (\partial_\rho A - 4\partial_\rho \chi)] = 0. \quad (17)$$

This defines a conserved quantity, which vanishes for DW solutions in six dimensions, for which the metric ds_6^2 in Eq. (7) has the warp factor defined by $\mathcal{A} \equiv A - \chi = 3\chi$ (or $A = 4\chi$).

III. CLASSES OF SOLUTIONS

Here, we introduce the three main classes of solutions that we study in the following. We explain the naming choices, before we exhibit the functional form of the solutions, because they introduce some mild abuse of language, driven mostly by analogy, which we want to alert the reader to. We start from solutions to the first-order equations derived from the superpotential formalism, along the lines of fake supergravity [102]. We call them supersymmetric solutions, despite the fact that there is no supersymmetry—the theory is bosonic. The reason for this naming convention is an analogy with top-down models derived from higher-dimensional supergravity, for which the first-order equations coincide with the Bogomol’nyi-Prasad-Sommerfield constraints.

The most important class of solutions of interest, and for which we compute the spectrum of fluctuations, later in the paper, is denoted as confining solutions, again with abuse of language. In models in which a lift to a higher-dimensional supergravity derived from a string theory exists, it might be possible to compute the Wilson loop, along the lines of other holographic models [103–108], to expose the area law expected from confinement. This being a bottom-up model, such calculation cannot be carried out, yet the solutions are completely smooth and introduce a mass gap in the spectrum of fluctuations, which are weaker requirements for the gravity dual of a confining theory.

Finally, we also introduce a set of singular backgrounds, that we call domain-wall solutions, because in six dimensions they take the form of Poincaré domain walls. There is again abuse of language: strictly speaking the singularity signifies that they should not be taken literally as background solutions and used with caution—but see Ref. [109]. Our reason for considering them is that, as we shall see, they teach us something important about the other classes of solutions and their stability.

A. UV expansions

All the solutions we work with have the same asymptotic behavior for large ρ : they approach the $\phi = 0$ critical point of \mathcal{V}_6 , with $\chi \simeq \frac{1}{3}\rho$ and $A \simeq \frac{4}{3}\rho$ (equivalently, $\mathcal{A} \simeq \rho$). Asymptotically in the UV, the gravity duals have common interpretations in terms of (relevant or marginal) deformations of the same five-dimensional CFT. We hence classify all the solutions in terms of a power expansion in the small parameter $z \equiv e^{-\rho}$. The expansion depends on five free parameters.

Two parameters are additive contributions to χ and A , which we denote χ_U and A_U , respectively. One free parameter appears in χ in the coefficient of the z^5 term, and we denote it as χ_5 . We fix an additive contribution to χ_5 so that if $A = 4\chi$ (as is the case for the DW solutions), then $\chi_5 = 0$. For generic values of Δ , the remaining two free parameters appear in the expansion of ϕ at orders z^Δ and $z^{5-\Delta}$, and we call ϕ_J (ϕ_V) the coefficient in front of the term with the smallest (largest) exponent Δ_J (Δ_V). The expansions take the generic form

$$\phi(z) = \phi_J z^{\Delta_J} + \dots + \phi_V z^{\Delta_V} + \dots, \quad (18)$$

$$\chi(z) = \chi_U - \frac{1}{3} \log(z) + \dots + (\chi_5 + \dots) z^5 + \dots, \quad (19)$$

$$A(z) = A_U - \frac{4}{3} \log(z) + \dots. \quad (20)$$

In the special case with $\Delta = 5/2$, for which the two independent parameters appear in front of the $z^{5/2}$ and $z^{5/2} \log(z)$ terms in the expansion of ϕ , we denote the former as ϕ_V , and the latter as ϕ_J . As we shall see, these

coefficients are very important in determining the physical properties of the solutions and their field-theory duals. For example, the free energy depends on a combination of $\phi_J\phi_V$ and χ_5 . We further note that, without loss of generality, one may restrict attention to solutions for which $A_U = 0 = \chi_U$.

The expansion depends nontrivially on Δ . For definiteness, we report here the case $\Delta = 3$, while more examples can be found in Appendix C:

$$\phi(z) = \phi_J z^2 + \phi_V z^3 - \frac{25}{48} \phi_J^3 z^6 - \frac{57}{80} \phi_J^2 \phi_V z^7 + \mathcal{O}(z^8), \quad (21)$$

$$\chi(z) = \chi_U - \frac{1}{3} \log(z) - \frac{1}{24} \phi_J^2 z^4 + \left(\chi_5 - \frac{2}{25} \phi_J \phi_V \right) z^5 - \frac{1}{24} \phi_V^2 z^6 + \mathcal{O}(z^8), \quad (22)$$

$$A(z) = A_U - \frac{4}{3} \log(z) - \frac{1}{6} \phi_J^2 z^4 + \left(\frac{1}{4} \chi_5 - \frac{8}{25} \phi_J \phi_V \right) z^5 - \frac{1}{6} \phi_V^2 z^6 + \mathcal{O}(z^8). \quad (23)$$

B. Supersymmetric solutions

As the scalar potential \mathcal{V}_6 is written in terms of a superpotential \mathcal{W}_6 , a special class of six-dimensional DW solutions [for which $A(\rho) = 4\chi(\rho) = \frac{4}{3}\mathcal{A}(\rho)$] is recovered by solving the first-order equations

$$\partial_\rho \mathcal{A} = -\frac{1}{2} \mathcal{W}_6 = 1 + \frac{\Delta}{4} \phi^2, \quad (24)$$

$$\partial_\rho \phi = \frac{\partial \mathcal{W}_6}{\partial \phi} = -\Delta \phi, \quad (25)$$

which, as anticipated, we call supersymmetric solutions:

$$\phi(\rho) = \phi_c e^{-\Delta \rho} = \phi_c z^\Delta, \quad (26)$$

$$\mathcal{A}(\rho) = \rho - \frac{1}{8} \phi_c^2 e^{-2\Delta \rho} = -\log(z) - \frac{1}{8} \phi_c^2 z^{2\Delta}. \quad (27)$$

Besides ϕ_c , a second, additive integration constant has been omitted from \mathcal{A} . We recover the AdS₆ geometry with $\phi_c = 0$.

C. Confining solutions

The aforementioned confining solutions are such that the circle parametrized by η shrinks to zero size at some point ρ_o of the radial direction ρ —which is hence bounded from below as $\rho_o < \rho_1 \leq \rho < \rho_2 \rightarrow +\infty$ —and are also completely regular and smooth, as the metric in six

dimensions has finite curvature invariants and there is no conical singularity. By power expanding near the end of space, for small $(\rho - \rho_o)$, we find that such solutions have the following form:

$$\phi(\rho) = \phi_I - \frac{1}{16} \Delta \phi_I (20 + \Delta(5\phi_I^2 - 4)) (\rho - \rho_o)^2 + \mathcal{O}((\rho - \rho_o)^4), \quad (28)$$

$$\chi(\rho) = \chi_I + \frac{1}{3} \log(\rho - \rho_o) + \frac{1}{288} (-80 + 8(\Delta - 5)\Delta \phi_I^2 - 5\Delta^2 \phi_I^4) (\rho - \rho_o)^2 + \mathcal{O}((\rho - \rho_o)^4), \quad (29)$$

$$A(\rho) = A_I + \frac{1}{3} \log(\rho - \rho_o) + \frac{7}{576} (80 + \Delta \phi_I^2 (40 + \Delta(5\phi_I^2 - 8))) (\rho - \rho_o)^2 + \mathcal{O}((\rho - \rho_o)^4), \quad (30)$$

where ϕ_I , χ_I , A_I , and ρ_o are integration constants.

The induced metric on the (ρ, η) submanifold is

$$ds_2^2 = d\rho^2 + e^{6\chi} d\eta^2 \simeq d\rho^2 + e^{6\chi_I} (\rho - \rho_o)^2 d\eta^2 + \dots, \quad (31)$$

which is the metric of the plane, provided η has periodicity 2π and we fix $\chi_I = 0$, to avoid a conical singularity.

As a side remark, when $\Delta = 0$, we can write the solution in closed form:

$$\phi(\rho) = \phi_I, \quad (32)$$

$$\chi(\rho) = \chi_o - \frac{1}{5} \log \left[\cosh \left(\frac{5}{2} (\rho - \rho_o) \right) \right] + \frac{1}{3} \log \left[\sinh \left(\frac{5}{2} (\rho - \rho_o) \right) \right], \quad (33)$$

$$A(\rho) = A_o + \frac{4}{15} \log[\sinh(5(\rho - \rho_o))] + \frac{1}{15} \log \left[\tanh \left(\frac{5}{2} (\rho - \rho_o) \right) \right], \quad (34)$$

where χ_o and A_o are additive integration constants.

The curvature invariants in six dimensions—the Ricci scalar $\mathcal{R} \equiv \mathcal{R}_6$, the Ricci tensor squared $\mathcal{R}_2^2 \equiv \mathcal{R}_{\hat{M}\hat{N}} \mathcal{R}_6^{\hat{M}\hat{N}}$, and the Riemann tensor squared $\mathcal{R}_4^2 \equiv \mathcal{R}_{\hat{M}\hat{N}\hat{R}\hat{S}} \mathcal{R}_6^{\hat{M}\hat{N}\hat{R}\hat{S}}$ —can be written in terms of the nontrivial quantity

$$d \equiv A - 4\chi, \quad (35)$$

which vanishes on the DW solutions. After using the equations of motion, we find the following [97]:

$$\mathcal{R} = 6\mathcal{V}_6 + 2(\partial_\rho \phi)^2, \quad (36)$$

$$\mathcal{R}_2^2 = 6\mathcal{V}_6^2 + 4\mathcal{V}_6(\partial_\rho \phi)^2 + 4(\partial_\rho \phi)^4, \quad (37)$$

$$\mathcal{R}_4^2 = \frac{1}{250} \left(32(\partial_\rho d)^2 \left(4\partial_\rho d \sqrt{36(\partial_\rho d)^2 + 15\sqrt{5}\sqrt{6R_2^2 - R^2 - 30R + 24(\partial_\rho d)^2}} \right. \right. \\ \left. \left. + 5\sqrt{5}\sqrt{6R_2^2 - R^2 - 10R} \right) - 25(\mathcal{R}^2 - 10\mathcal{R}_2^2) \right). \quad (38)$$

All of these quantities are finite when $\rho \rightarrow \rho_o$, as can be seen by explicitly using the IR expansions:

$$\lim_{\rho \rightarrow \rho_o} \mathcal{R} = -30 - 3\Delta(5 - \Delta)\phi_I^2 - \frac{15\Delta^2}{8}\phi_I^4, \quad (39)$$

$$\lim_{\rho \rightarrow \rho_o} \mathcal{R}_2^2 = \frac{1}{6} (\lim_{\rho \rightarrow \rho_o} \mathcal{R})^2, \quad (40)$$

$$\lim_{\rho \rightarrow \rho_o} \mathcal{R}_4^2 = \frac{1}{3} (\lim_{\rho \rightarrow \rho_o} \mathcal{R})^2. \quad (41)$$

Interestingly though, as long as $\Delta \neq 0$, all these invariants diverge for $\phi_I \rightarrow \infty$, suggesting *a priori* that we should not be allowed to take the value of ϕ_I to be arbitrarily large.

D. Singular domain-wall solutions

The last class of solutions of interest to this paper is given by singular DW solutions. They obey the DW ansatz $A = 4\chi = \frac{4}{3}\mathcal{A}$. Their IR expansion depends explicitly on Δ and reads as follows:

$$\phi(\rho) = \phi_I - \sqrt{\frac{2}{5}} \log(\rho - \rho_o) + \frac{(\rho - \rho_o)^2}{25920} (2\sqrt{10}(6\Delta \log(\rho - \rho_o)(3 \log(\rho - \rho_o)(\Delta \log(\rho - \rho_o)(3 \log(\rho - \rho_o) + 2) \\ - 23\Delta + 60) + 37\Delta + 60) - \Delta(47\Delta + 660) + 5400) \\ + 15\Delta\phi_I(-60\phi_I^2(6\Delta \log(\rho - \rho_o) + \Delta) + 6\sqrt{10}\phi_I(6\Delta \log(\rho - \rho_o)(3 \log(\rho - \rho_o) + 1) \\ - 23\Delta + 60) - 4(6 \log(\rho - \rho_o)(3\Delta \log(\rho - \rho_o)(2 \log(\rho - \rho_o) + 1) \\ - 23\Delta + 60) + 37\Delta + 60) + 45\sqrt{10}\Delta\phi_I^3)) + \mathcal{O}((\rho - \rho_o)^4), \quad (42)$$

$$\mathcal{A}(\rho) = \frac{1}{5} \log(\rho - \rho_o) + \frac{(\rho - \rho_o)^2}{12960} (2(6\Delta \log(\rho - \rho_o)(3 \log(\rho - \rho_o)(\Delta \log(\rho - \rho_o)(3 \log(\rho - \rho_o) - 10) \\ + 7\Delta + 60) - 5(\Delta + 60)) + (1140 - 17\Delta)\Delta + 5400) \\ + 3\Delta\phi_I(2\sqrt{10}(5(\Delta + 60) - 6 \log(\rho - \rho_o)(3\Delta \log(\rho - \rho_o)(2 \log(\rho - \rho_o) - 5) + 7\Delta + 60)) \\ + 15\phi_I(2(6\Delta \log(\rho - \rho_o)(3 \log(\rho - \rho_o) - 5) + 7\Delta + 60) \\ + \Delta\phi_I(2\sqrt{10}(5 - 6 \log(\rho - \rho_o)) + 15\phi_I)))) + \mathcal{O}((\rho - \rho_o)^4). \quad (43)$$

In these expressions, ϕ_I is an integration constant, and without loss of generality we omitted an additive integration constant in \mathcal{A} . We recall that the system of equations is symmetric under the change $\phi \rightarrow -\phi$; hence, a second branch of solutions can be obtained by just changing the sign of ϕ .

These solutions are singular at the end of space. Their nature in the gravity theory is unclear, and they do not admit a transparent field-theory interpretation. In particular, we do not compute the spectrum of their fluctuations—otherwise interpreted in terms of bound states in a putative dual theory—as there is no clear sense in which this would provide information about observable

quantities. Yet, we do compute their free energy later in the paper, because, as we shall see, for some choices of parameters, solutions of this class are energetically favored over the confining ones. We will come back to this discussion in due time; we only anticipate here that this finding will force us to restrict our physics discussions of the confining solutions to a subregion of the full parameter space.

IV. MASS SPECTRUM OF FLUCTUATIONS

In this section, we restrict our attention to the confining solutions only. Given a background solution in the

gravity theory, one can linearize the equations of motion of small fluctuations around it. The resulting mass spectra of fluctuations of the bosonic fields correspond, following the gauge-gravity duality dictionary, to spin-0, 1, 2 composite particles in the (putative) dual confining field theory in four dimensions. To perform the calculations, we adopt the gauge-invariant formalism developed in Refs. [81–85]. We start from the scalar fluctuations $\mathbf{a}^a = \mathbf{a}^a(q, \rho)$, where q^μ is the four-momentum, which obey the following equations (see also Appendix A 1):

$$[\partial_\rho^2 + (4\partial_\rho A - \partial_\rho \chi)\partial_\rho - e^{2\chi-2A}q^2]\mathbf{a}^a - e^{2\chi}\mathcal{X}_c^a \mathbf{a}^c = 0. \quad (44)$$

Because the sigma-model metric is simply $G_{ab} = \text{diag}(1, 6)$, in the basis $\Phi^a = \{\phi, \chi\}$, the sigma-model connection vanishes, greatly simplifying the equations of motion, as \mathcal{X}_c^a reads as follows:

$$\begin{aligned} \mathcal{X}_c^a \equiv & \frac{\partial}{\partial \Phi^c} \left(G^{ab} \frac{\partial(e^{-2\chi}\mathcal{V}_6)}{\partial \Phi^b} \right) \\ & + \frac{4}{3\partial_\rho A} \left[\partial_\rho \Phi^a \frac{\partial(e^{-2\chi}\mathcal{V}_6)}{\partial \Phi^c} + G^{ab} \frac{\partial(e^{-2\chi}\mathcal{V}_6)}{\partial \Phi^b} \partial_\rho \Phi^d G_{dc} \right] \\ & + \frac{16(e^{-2\chi}\mathcal{V}_6)}{9(\partial_\rho A)^2} \partial_\rho \Phi^a \partial_\rho \Phi^b G_{bc}. \end{aligned} \quad (45)$$

In all these expressions, the functions A , $\Phi^a = \{\phi, \chi\}$, and \mathcal{V}_6 are evaluated on the background.

A discrete spectrum can be found by imposing the following boundary conditions¹:

$$\begin{aligned} & e^{-2\chi} \partial_\rho \Phi^c \partial_\rho \Phi^d G_{db} \partial_\rho \mathbf{a}^b \Big|_{\rho_i} \\ & = \left[\frac{3\partial_\rho A}{2} e^{-2A} q^2 \delta^c_b + \partial_\rho \Phi^c \left(\frac{4\mathcal{V}_6}{3\partial_\rho A} \partial_\rho \Phi^d G_{db} + \frac{\partial \mathcal{V}_6}{\partial \Phi^b} \right) \right] \mathbf{a}^b \Big|_{\rho_i}. \end{aligned} \quad (46)$$

Physical composite states in the dual theory have mass $M^2 = -q^2$, corresponding to choices of q^2 for which the boundary conditions at the two boundaries can be satisfied simultaneously.

The equations of motion for the (transverse and traceless) tensor fluctuations $e^\mu{}_\nu$ are the following [80]:

$$0 = [\partial_\rho^2 + (4\partial_\rho A - \partial_\rho \chi)\partial_\rho - e^{2\chi-2A}q^2]e^\mu{}_\nu, \quad (47)$$

while for the vector χ_M one looks at the gauge-invariant transverse polarizations, which obey the bulk equation

$$0 = P^{\mu\nu}[\partial_\rho^2 + (2\partial_\rho A + 7\partial_\rho \chi)\partial_\rho - e^{2\chi-2A}q^2]\chi_\nu, \quad (48)$$

¹The equivalent form of the boundary conditions given in Eq. (14) of Ref. [70] is convenient in numerical implementations.

where $P^{\mu\nu} \equiv \eta^{\mu\nu} - \frac{q^\mu q^\nu}{q^2}$. To compute the spectrum of masses, $M > 0$, of the bound states in the dual confining theory, one can impose Neumann boundary conditions on these two kinds of fluctuations.

The physical results can be recovered by first computing the spectrum for finite values of ρ_1 and ρ_2 and then by repeating the calculations to extrapolate toward the limits $\rho_1 \rightarrow \rho_o$ and $\rho_2 \rightarrow +\infty$ [79,80,85]. Equivalent results can be obtained with an alternative numerical strategy, which improves the convergence in such limits by making use of the UV and IR expansions of the fluctuations. One decomposes them in dominant and subdominant modes, notices that the boundary conditions are equivalent to suppressing the dominant fluctuations, and then matches the solutions to the expansions, evaluated at finite $\rho_{1,2}$. This nontrivial process requires knowing the appropriate expansions at high orders in the small parameters (z in the UV and $\rho - \rho_o$ in the IR) but has the great advantage that one does not require extending the background solutions of the nonlinear equations of motion to numerically challenging values at large (small) $\rho - \rho_o$. This strategy was successful in the study of the Klebanov-Strassler system [83] and its baryonic branch [71,72], and we adopt it here. We report IR expansions, and one example of UV expansions, for the fluctuations in Appendix D.

As explained and exemplified in Ref. [86], as well as Appendix E, the probe approximation is equivalent to ignoring the coupling of the states to the trace of the energy-momentum tensor and hence discarding the mixing in the physical states with the dilaton field. This approximation fails to reproduce the mass of states with substantial overlap with the dilatation operator. When such states are light, they should hence be interpreted as approximate dilatons, turning this approximation into a diagnostic tool for the identification of approximate dilatons. We will perform the analysis of the mass spectrum in the probe approximation only for the choice of $\Delta = 5/2$, which turns out to be the most interesting in the context of this paper.

The mass spectra are computed numerically, and we report the results in Figs. 1–4, for a few significant choices of Δ . For each of them, we compute the spectrum of spin-0, spin-1, and spin-2 fluctuations. We conveniently normalize the spectra so that the lightest tensor state has mass $M = 1$. For each value of Δ , we check the convergence of the spectrum, as a function of ρ_1 and ρ_2 independently, and report numerical results obtained with choices for which the dependence on the two cutoffs can be neglected in respect to our numerical accuracy goal of 0.5%. Finally, we find it convenient to report in the plots also the critical value of $\phi_I(c)$, obtained from the numerical study of the free energy, as detailed in the next section.

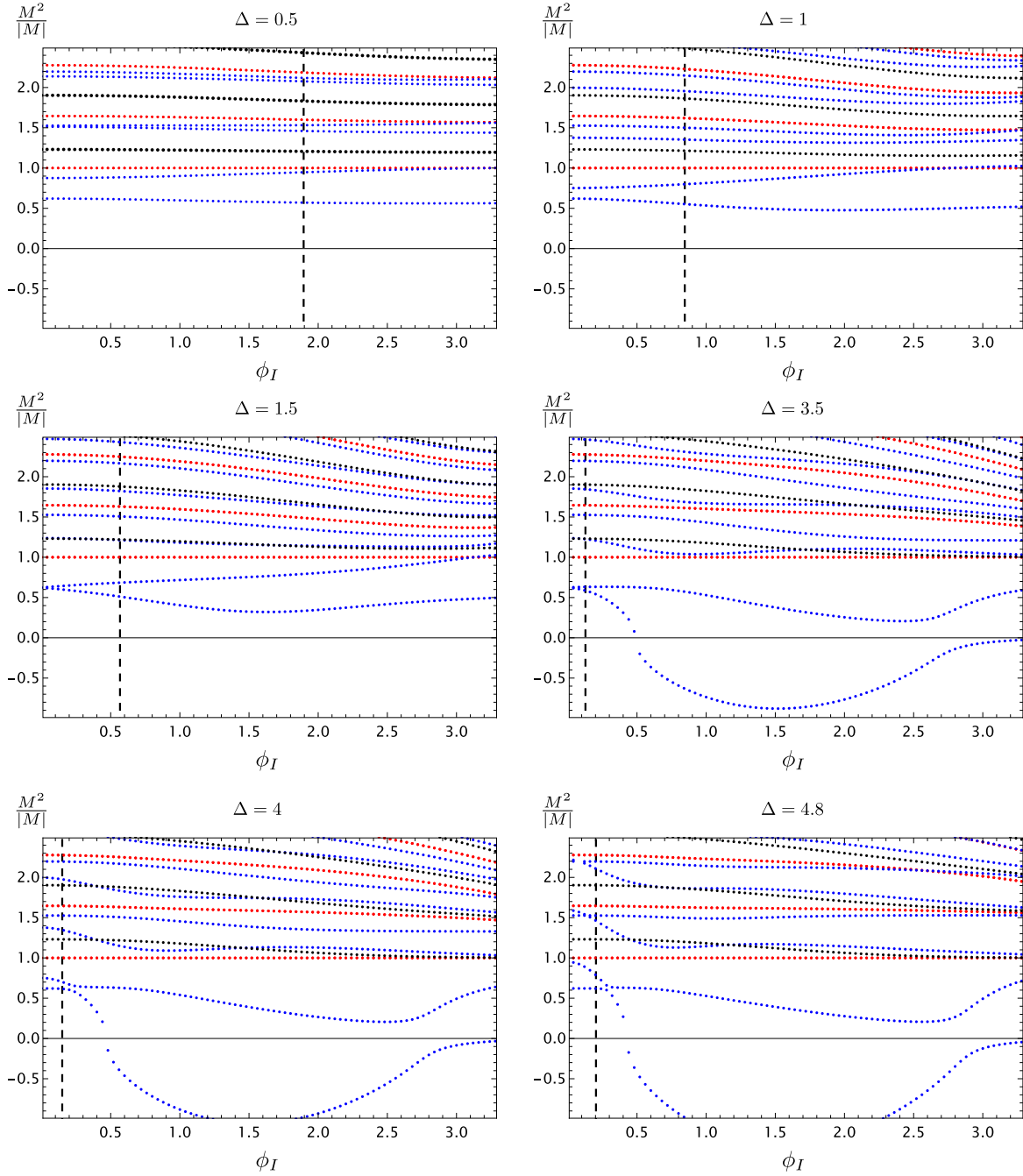


FIG. 1. Mass spectrum $\frac{M^2}{|M|}$ of fluctuations, computed for confining backgrounds, with various choices of Δ , as a function of the IR parameter ϕ_I . For each Δ , we show the spectrum of spin-0 (blue dots), spin-1 (black dots), and spin-2 (red dots) states. The values of the IR and UV cutoffs in the calculations are, respectively, given by $\rho_1 - \rho_o = 10^{-9}$ and $\rho_2 - \rho_o = 5$. All masses are normalized to the mass of the lightest spin-2 state. The vertical dashed lines denote the critical value $\phi_I(c)$.

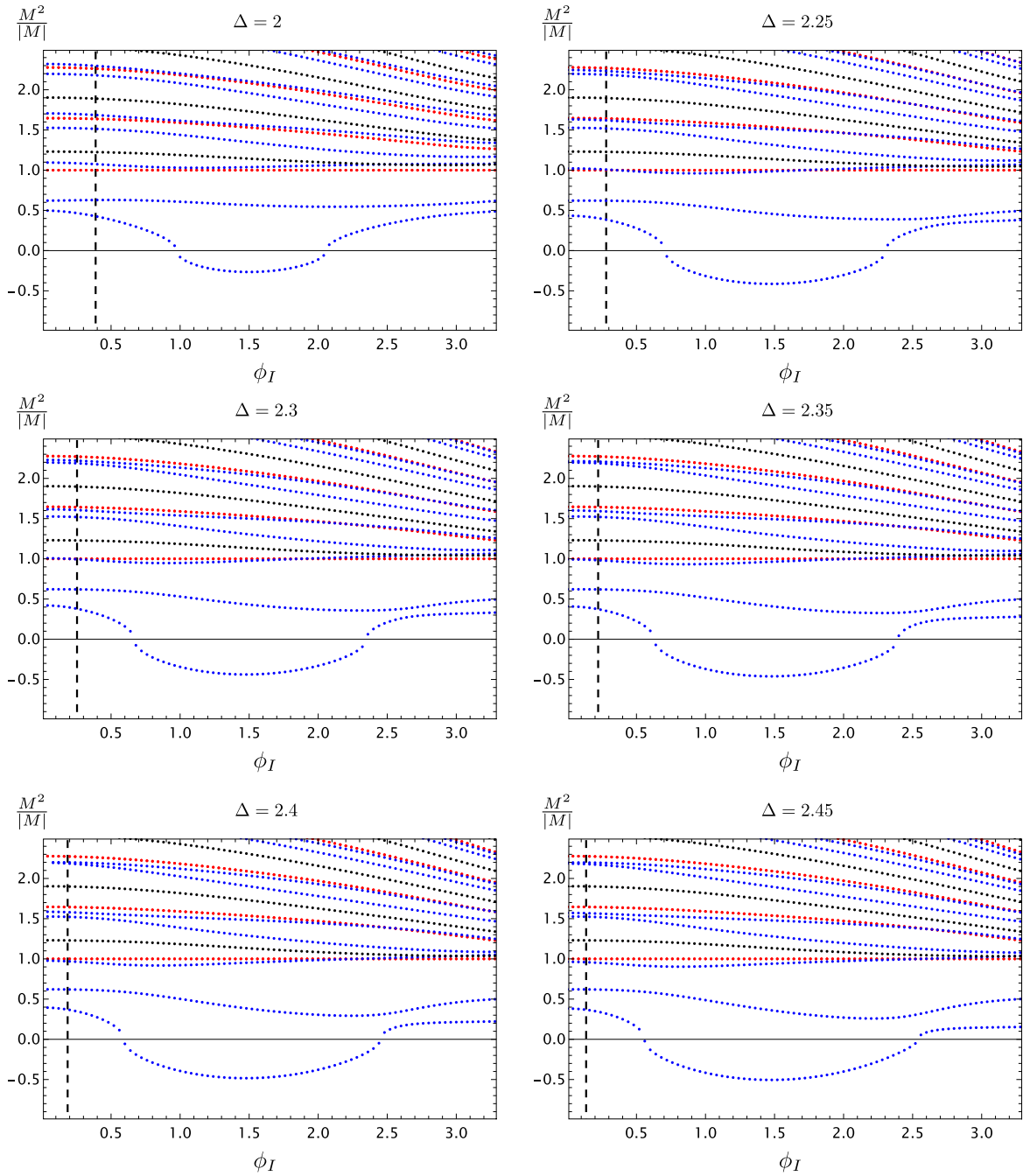


FIG. 2. Mass spectrum $\frac{M^2}{|M|}$ of fluctuations, computed for confining backgrounds, with various choices of Δ , as a function of the IR parameter ϕ_I . For each Δ , we show the spectrum of spin-0 (blue dots), spin-1 (black dots), and spin-2 (red dots) states. The values of the IR and UV cutoffs in the calculations are, respectively, given by $\rho_1 - \rho_o = 10^{-9}$ and $\rho_2 - \rho_o = 5$. All masses are normalized to the mass of the lightest spin-2 state. The vertical dashed lines denote the critical value $\phi_I(c)$.

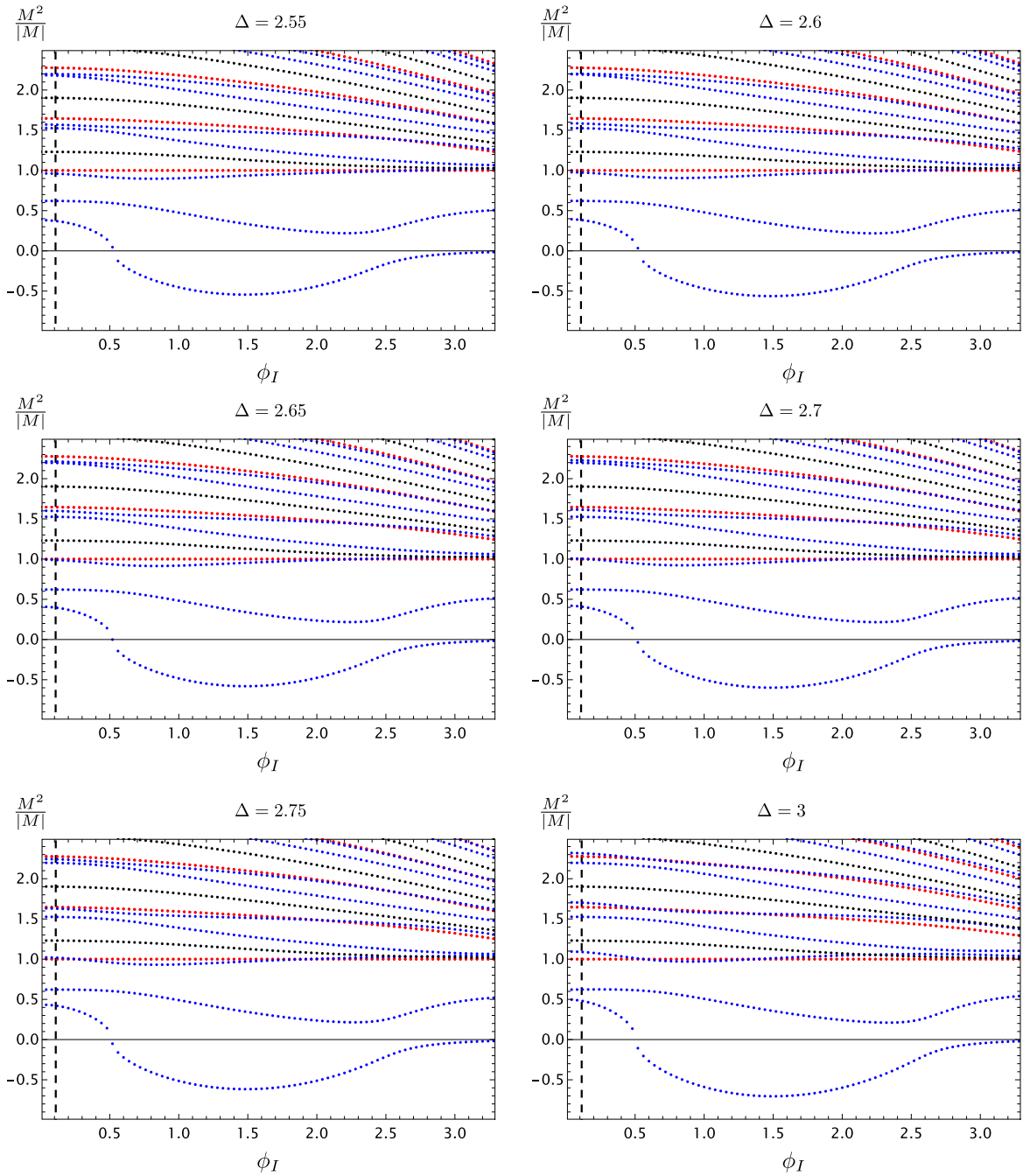


FIG. 3. Mass spectrum $\frac{M^2}{|M|}$ of fluctuations, computed for confining backgrounds, with various choices of Δ , as a function of the IR parameter ϕ_I . For each Δ , we show the spectrum of spin-0 (blue dots), spin-1 (black dots), and spin-2 (red dots) states. The values of the IR and UV cutoffs in the calculations are, respectively, given by $\rho_1 - \rho_o = 10^{-9}$ and $\rho_2 - \rho_o = 5$. All masses are normalized to the mass of the lightest spin-2 state. The vertical dashed lines denote the critical value $\phi_I(c)$.

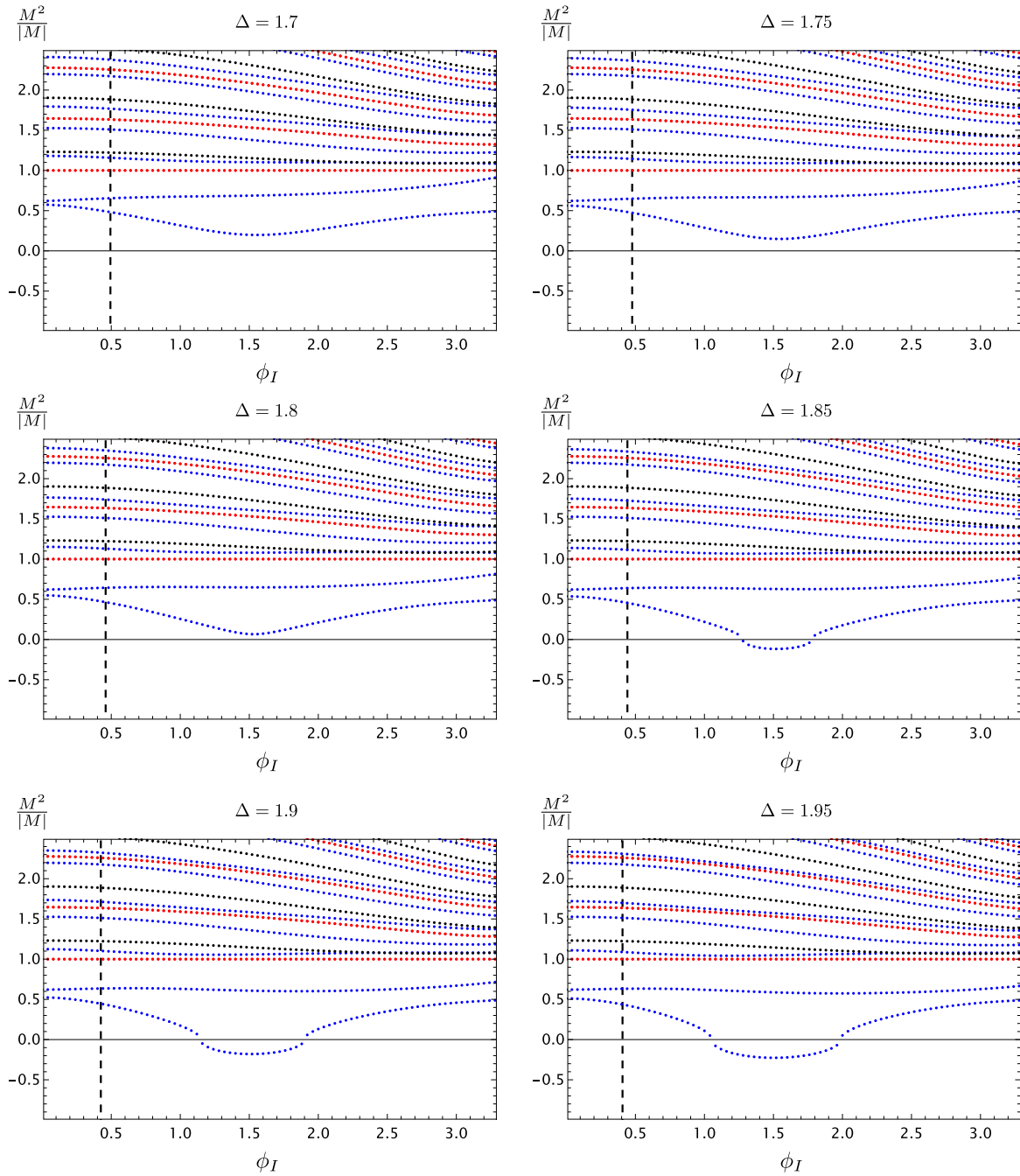


FIG. 4. Mass spectrum $\frac{M^2}{|M|}$ of fluctuations, computed for confining backgrounds, with various choices of Δ , as a function of the IR parameter ϕ_I . For each Δ , we show the spectrum of spin-0 (blue dots), spin-1 (black dots), and spin-2 (red dots) states. The values of the IR and UV cutoffs in the calculations are, respectively, given by $\rho_1 - \rho_o = 10^{-9}$ and $\rho_2 - \rho_o = 5$. All masses are normalized to the mass of the lightest spin-2 state. The vertical dashed lines denote the critical value $\phi_I(c)$.

V. FREE ENERGY

The free energy density is given by the following expression:

$$\mathcal{F} = - \lim_{\rho_2 \rightarrow +\infty} e^{4A-\chi} \left(\frac{3}{2} \partial_\rho A + \mathcal{W}_2 \right) \Big|_{\rho_2}, \quad (49)$$

where $\mathcal{W}_2 = \mathcal{W}_6$ if $\Delta < 5/2$ or $\mathcal{W}_2 = \bar{\mathcal{W}}_6$ if $\Delta > 5/2$. This expression has been obtained by adapting the results in Ref. [97]; it includes the contribution of the bulk action, evaluated by imposing the equations of motion, the contribution of the boundary terms in the action, and the appropriate UV-localized counterterm \mathcal{W}_2 , which is required by the rules of holographic renormalization [87–89], as it removes the UV divergences. The conservation law in Eq. (17) has been used to evaluate at ρ_2 (the UV boundary) a term naturally defined at ρ_1 (the IR boundary).

For each choice of the parameter Δ , one expresses \mathcal{F} in terms of the coefficients appearing in the UV expansion of the background, which can be extracted by matching the expansions to numerical solutions. Care must be taken to obtain results that converge as $\rho_2 \rightarrow +\infty$. We empirically find that, for $\Delta < 5/2$, the free energy density is

$$\mathcal{F} = -\frac{1}{40} e^{4A_U - \chi_U} \left(16\Delta \left(\frac{5}{2} - \Delta \right) \phi_J \phi_V - 75\chi_5 \right), \quad (50)$$

while for $\Delta > 5/2$ —and retaining in $\bar{\mathcal{W}}_6$ a sufficient number of terms to ensure cancellation of all the divergences—the free energy density is

$$\mathcal{F} = -\frac{1}{40} e^{4A_U - \chi_U} \left(16(\Delta - 5) \left(\frac{5}{2} - \Delta \right) \phi_J \phi_V - 75\chi_5 \right). \quad (51)$$

We explicitly checked that this expression is accurate for all values of Δ considered in this paper. In the special case in which the operator has dimension $\Delta = 5/2$, we find that

$$\mathcal{W}_2 = -2 - \frac{5}{4} \phi^2 \left(1 + \frac{2}{5 \log(kz)} \right), \quad (52)$$

and the free energy density is

$$\mathcal{F} = \frac{1}{40} e^{4A_U - \chi_U} (20\phi_J \phi_V - 4\phi_J^2 + 75\chi_5 - 20\phi_J^2 \log(k)). \quad (53)$$

The appearance of a logarithm introduces a residual scheme dependence, encoded in the parameter k . In the following, we make the choice $k = \Lambda$.

Following Refs. [97–99], we find it convenient to define a scale Λ as follows [90]:

$$\Lambda^{-1} \equiv \int_{\rho_o}^{\infty} d\rho e^{\chi(\rho) - A(\rho)}, \quad (54)$$

with ρ_o the end of space—other choices are admissible, but this choice makes contact with earlier studies, where it has been shown that it allows one to compare the confining and DW classes of solutions. We then express all of the quantities of interest in units of such scale Λ , by defining the rescaled free energy density

$$\hat{\mathcal{F}} \equiv \frac{\mathcal{F}}{\Lambda^5} \quad (55)$$

and the rescaled source as

$$\hat{\phi}_J \equiv \frac{\phi_J}{\Lambda^{\Delta_J}}, \quad (56)$$

where Δ_J is the dimension of the deforming coefficient (source) associated with the dual operator of dimension $\Delta_V \equiv 5 - \Delta_J$. We hence define also the rescaled condensates to be

$$\hat{\phi}_V \equiv \frac{\phi_V}{\Lambda^{\Delta_V}}, \quad (57)$$

$$\hat{\chi}_5 \equiv \frac{\chi_5}{\Lambda^5}. \quad (58)$$

Given a background solution, in order to compute the free energy we proceed as follows. First, we match it to the UV expansions and determine coefficients $A_U, \chi_U, \phi_J, \phi_V$, and χ_5 . We then shift additively both the radial coordinate ρ and the definition of the function $A(\rho)$, to impose the constraints $A_U = 0 = \chi_U$. We repeat the determination of the coefficients and enter the results in the expression for the free energy density. We compute the scale Λ for each background—after the aforementioned shifts of ρ and $A(\rho)$ —and finally plot the resulting, rescaled quantities. Examples are shown in Figs. 5–8. We do so for both confining and DW singular solutions and show them together for each Δ .

By inspection of the figures, we see the emergence of a common pattern; in all cases, the confining solutions minimize the free energy $\hat{\mathcal{F}}$ for small choices of the source $|\hat{\phi}_J|$, while the singular, DW solutions have the lowest $\hat{\mathcal{F}}$ for larger values of the source. There is a critical value of $|\hat{\phi}_J(c)|$, corresponding to a critical value of the IR parameter $|\phi_I(c)|$, where a first-order phase transition occurs. For $|\phi_I| \leq |\phi_I(c)|$, the confining solutions can be physically realized, while for $|\phi_I| > |\phi_I(c)|$, the physical solution is unknown, so that we are forced to discard these latter regions of parameter space. We are not claiming that the singular solutions are physically realized but simply that some other

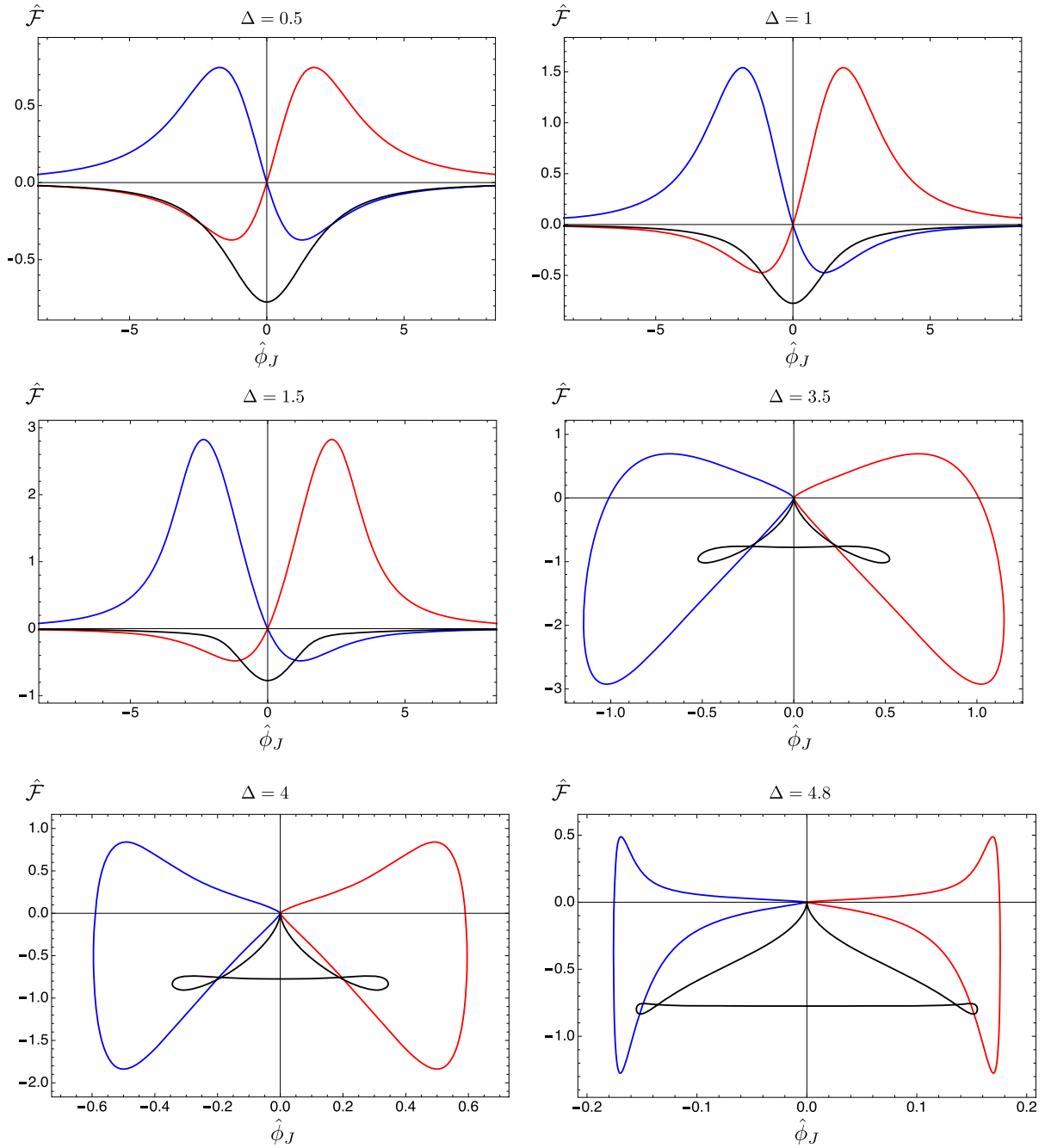


FIG. 5. The free energy density $\hat{\mathcal{F}}$ as a function of the source $\hat{\phi}_J$, in units of the scale Λ , for various choices of Δ . The black curve denotes the confining solutions, while the red and blue solutions are singular domain-wall ones.

branch of solutions, not identified in this study, might exist and take over the long-distance dynamics in these cases.

When inspected more closely, the figures show other interesting features. For $\Delta \geq 5/2$, both confining and singular solutions cease to exist above some value of $|\hat{\phi}_J(\max)| > |\hat{\phi}_J(c)|$. As we already know (from the aforementioned arguments) that, at large $|\hat{\phi}_J| > |\hat{\phi}_J(c)|$, another branch of solutions must exist (possibly in a more complete theory), this is not a particularly problematic

finding. While this finding agrees with the results of the analysis of three distinct examples of top-down holographic models, reported in Refs. [97–99], it is interesting that this feature is absent for $\Delta < 5/2$, in which case confining and singular solutions exist for any choices of $\hat{\phi}_J$.

In thermodynamics, one can use the concavity theorems to discuss the stability of possible solutions, determined on the basis of the shape of the functional dependence of the free energy on the control parameters. These arguments do

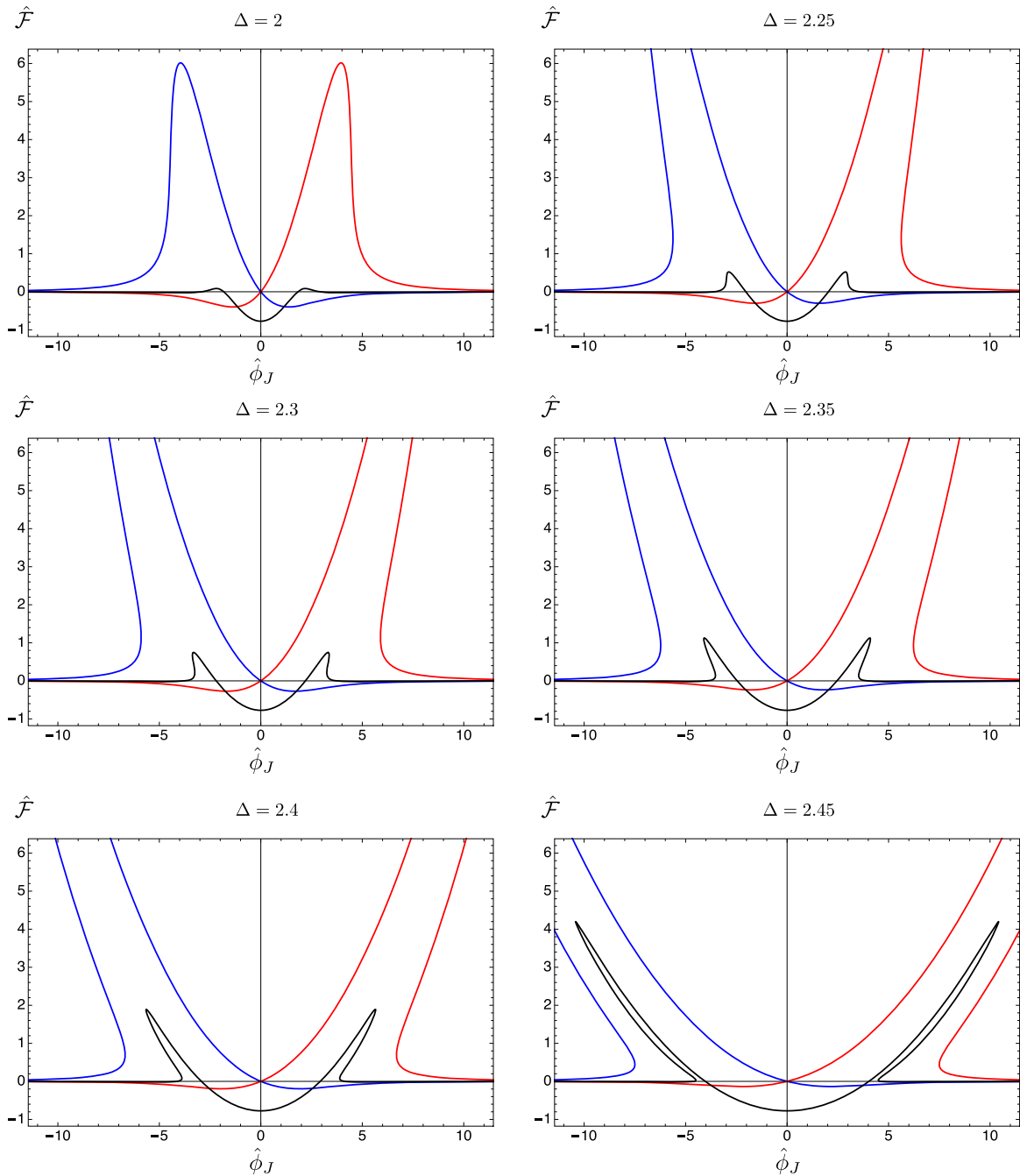


FIG. 6. The free energy density $\hat{\mathcal{F}}$ as a function of the source $\hat{\phi}_J$, in units of the scale Λ , for various choices of Δ . The black curve denotes the confining solutions, while the red and blue solutions are singular domain-wall ones.

not transfer directly to the case in question because of the presence of divergences and scheme dependences (see also Ref. [110] for examples of similar considerations in a different context), and caution has to be exercised. Yet, by comparing Figs. 5–8 with Figs. 1–4, one notices the following.

(i) A tachyon exists in the spectra of confining theories for values of $\Delta \gtrsim 1.8$ but only in a portion of parameter space (equivalently, for some range of ϕ_I).

(ii) The portion of parameter space in which the tachyon appears is always past the phase transition.

(iii) There is a region of parameter space over which the mass of the lightest scalar is parametrically small, near the point at which it turns tachyonic. But once more this happens only past the phase transition, in regions in which the confining solutions are, at best, metastable.

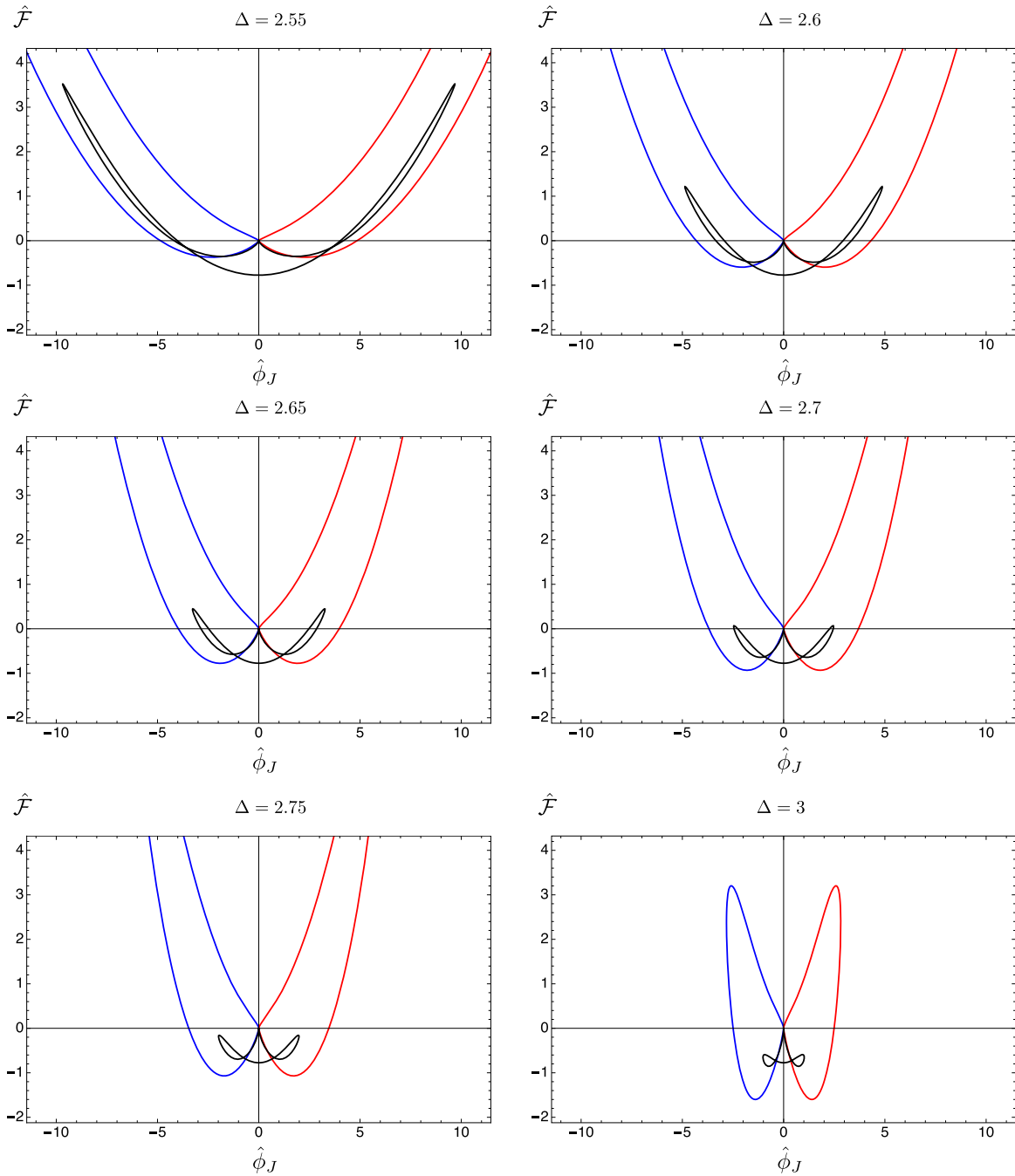


FIG. 7. The free energy density $\hat{\mathcal{F}}$ as a function of the source $\hat{\phi}_J$, in units of the scale Λ , for various choices of Δ . The black curve denotes the confining solutions, while the red and blue solutions are singular domain-wall ones.

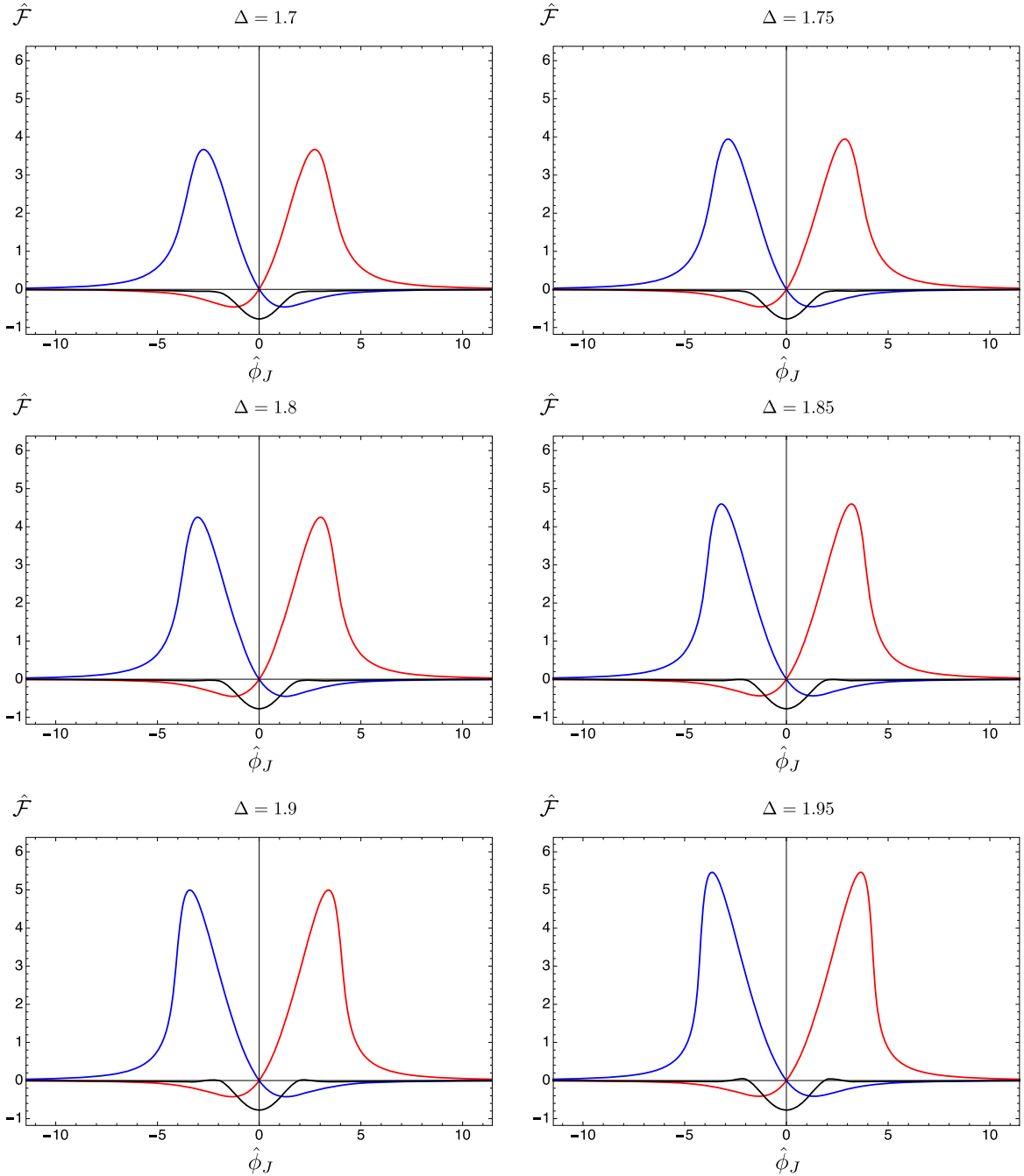


FIG. 8. The free energy density $\hat{\mathcal{F}}$ as a function of the source $\hat{\phi}_J$, in units of the scale Λ , for various choices of Δ . The black curve denotes the confining solutions, while the red and blue solutions are singular domain-wall ones.

We performed an extensive study of the free energy for values of $\Delta \simeq 1.8$, nearby where the tachyon appears—see also the details in Appendix F. We find that the free energy of the confining backgrounds is a monotonic function for Δ below $\Delta \simeq 1.7$. As expected, the relation between the behavior of \mathcal{F} and the appearance a tachyon is not precise, and furthermore these features always appear in a region of parameter space that has already been excluded, on the basis of earlier considerations.

We hence report on this feature, for completeness, but do not explore it any further.

VI. SUMMARY

We collect in Table I our numerical results: for representative values of Δ , we tabulate the critical parameters $\hat{\phi}_J(c)$ (source) and $\phi_I(c)$ (IR asymptotic value of ϕ), the mass of the lightest scalar $M(c)$ (in units of the mass of the

TABLE I. Summary table of our results. For each Δ , we report the critical value of the normalized source $\hat{\phi}_J(c)$ at the phase transition, the critical value of the IR expansion parameter $\phi_I(c)$, and the value of the mass $M(c)$ of the lightest scalar state at the transition—expressed in units of the mass of the lightest spin-2 state for the same choices of parameters. For completeness, we also report the value of the two parameters linked to the condensates in the dual field theory: $\hat{\phi}_V(c)$ and $\hat{\chi}_5(c)$.

Δ	$\hat{\phi}_J(c)$	$\phi_I(c)$	$M(c)$	$\hat{\phi}_V(c)$	$\hat{\chi}_5(c)$
0.50	2.373	1.89	0.571	-0.063	-0.176
1.00	1.149	0.845	0.553	-0.208	-0.328
1.50	0.990	0.567	0.512	-0.369	-0.368
1.70	1.010	0.494	0.482	-0.471	-0.377
1.75	1.022	0.477	0.473	-0.504	-0.380
1.80	1.038	0.459	0.464	-0.539	-0.382
1.85	1.059	0.442	0.455	-0.579	-0.384
1.90	1.084	0.424	0.446	-0.625	-0.386
1.95	1.115	0.407	0.436	-0.677	-0.388
2.00	1.153	0.388	0.427	-0.736	-0.390
2.25	1.567	0.281	0.385	-1.276	-0.401
2.30	1.756	0.254	0.379	-1.496	-0.403
2.35	2.045	0.223	0.374	-1.821	-0.405
2.40	2.554	0.186	0.370	-2.371	-0.408
2.45	3.748	0.136	0.367	-3.618	-0.410
2.49	8.750	0.063	0.368	-8.691	-0.412
2.499	27.82	0.020	0.369	-27.80	-0.413
2.50	-0.295	0.107	0.359	0.439	-0.411
2.501	147.3	0.107	0.359	-147.2	-0.411
2.51	14.79	0.107	0.362	-14.69	-0.411
2.55	3.001	0.108	0.372	-2.899	-0.411
2.60	1.528	0.108	0.384	-1.426	-0.411
2.65	1.038	0.108	0.397	-0.935	-0.411
2.70	0.793	0.109	0.409	-0.689	-0.411
2.75	0.647	0.109	0.421	-0.542	-0.411
3.00	0.358	0.113	0.481	-0.246	-0.411
3.50	0.225	0.127	0.586	-0.068	-0.411
4.00	0.189	0.150	0.616	-0.102	-0.410
4.80	0.136	0.204	0.620	-0.179	-0.410

lightest tensor), in proximity of the transition. For completeness, we also list the value of the two parameters representing the condensates in the dual field theory: $\hat{\phi}_V(c)$ and $\hat{\chi}_5(c)$. We show in Fig. 9 the mass spectrum and free energy for the $\Delta = 5/2$ case, and in Fig. 10 we display the mass spectrum computed at the critical value $\phi_I(c)$, for each choice of Δ .

The main results of the paper can be summarized as follows. The model allows us to study the spectrum and the free energy for any generic value of the parameter Δ , which is equal either to the dimensionality of the coupling deforming the dual CFT or to the associated condensate. Furthermore, for each Δ we restrict attention to regular backgrounds, the dual field theory of which has a mass gap and a discrete spectrum of bound states. These solutions of

the gravity equations of motion in five dimensions lift to completely regular and smooth solutions in six dimensions and admit an end of space in the radial direction $\rho > \rho_0$. We compute the spectrum of fluctuations of solutions of this type, which with abuse of notation we call *confining*. We find that for all values of the parameter $0 < \Delta < 5$ that we studied, there exists a first-order phase transition, that bounds from above the source associated with the scalar field ϕ . This is demonstrated by the existence of domain-wall solutions in six dimensions that, for large enough values of the deforming parameters, are energetically favored (despite being singular) over the confining ones. We find that for $\Delta \gtrsim 1.8$, the mass spectrum contains a tachyon, provided the deforming parameter is large enough. But this tachyon always appears only in an unphysical portion of parameter space, well beyond the phase transition. Conversely, in the physical portion of parameter space, all fluctuations have positive $M^2 > 0$ and are never parametrically light.

By inspecting Figs. 1–4, we notice that the mass of the lightest state in the spectrum, in units of the mass of the lightest tensor, becomes smaller when the source increases toward its critical value. Hence, the minimum value $M(c)$ of the mass of the lightest scalar is found in immediate proximity of the transition. For each choice of Δ , we compute the mass spectrum of bound states of the dual theory precisely at the phase transition point, which is displayed in Fig. 10. We find two interesting, unexpected features, which we highlight in closing this section.

First, the mass of the lightest scalar state has a minimum in proximity of $\Delta = 5/2$, in which case the mass of such state is approximately one-third of the mass of the tensor. We show explicitly in the top panel of Fig. 9 the mass spectrum computed in the probe approximation, which shows significant disagreement with the mass of the lightest scalar for large values of ϕ_I . In this case, the lightest scalar particle has a substantial overlap with the dilaton [86]. Unfortunately, this feature appears only inside the metastable (or tachyonic) region(s) of parameter space, while the probe approximation captures well the mass of the lightest scalar in the physical region, when $|\phi_I| \leq |\phi_I(c)|$.

Second, this summary plot displays a peculiar discontinuity at $\Delta = 5/2$ (see the inset of Fig. 10). The numerical value for the mass of the lightest scalar at $\Delta = 5/2$ aligns well with those obtained for $\Delta > 5/2$ and is the absolute minimum of the mass. However, the sequence of masses of the lightest scalar state one obtains for $\Delta < 5/2$ converges to a slightly higher value. We do not know why this second feature emerges and highlight to the reader the intrinsic numerical difficulty of some of the analysis we carried out. Yet, this discontinuity is a small effect, when compared to the much more significant first feature we found, namely that the mass of the lightest scalar is minimized for $\Delta = 5/2$.

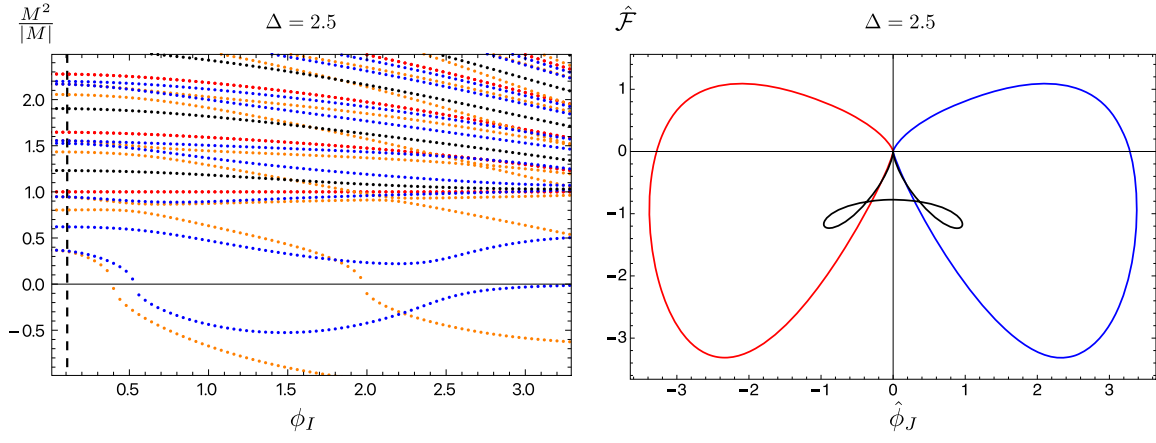


FIG. 9. The mass spectrum of fluctuations for $\Delta = 5/2$, displaying the spin-0 (blue dots), spin-1 (black dots), and spin-2 (red dots) states, in units of the mass of the lightest spin-2 state (left panel). The spectrum also includes the masses of the scalars computed in the probe approximation (orange dots), for comparison with the complete calculation (blue dots). The values of the IR and UV cutoffs in the calculations are, respectively, given by $\rho_1 - \rho_o = 10^{-9}$ and $\rho_2 - \rho_o = 5$. The (normalized) free energy density $\hat{\mathcal{F}}$, as a function of the source $\hat{\phi}_J$, for $\Delta = 5/2$ (right panel). The black curve denotes the confining solutions, while the red and blue solutions are singular domain-wall ones. The vertical, dashed line in the left panel indicates the position of the first-order phase transition evident in the right panel.

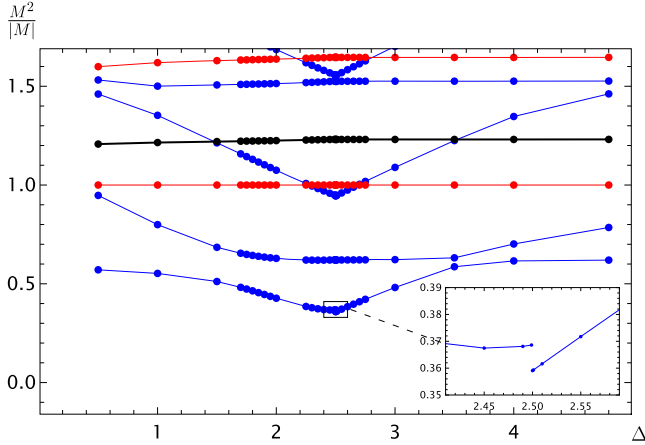


FIG. 10. The mass spectrum of fluctuations of the gravity theory (corresponding to the bound states of the dual field theory) evaluated at the critical $\phi_I(c)$ for each choice of Δ . We display the spin-0 (blue dots), spin-1 (black dots), and spin-2 (red dots) states. The values of the IR and UV cutoffs in the calculations are, respectively, given by $\rho_1 - \rho_o = 10^{-9}$ and $\rho_2 - \rho_o = 5$. All masses are normalized to the mass of the lightest spin-2 state.

VII. OUTLOOK

In a broad class of bottom-up holographic models, in which the background geometry ends smoothly, so as to introduce a mass gap in the dual field theory in a way that mimics a confining theory, and furthermore in the presence of an additional deformation (and the corresponding condensate), we found evidence of the presence of a first-order phase transition. The nature of the model allows one to treat Δ , the dimensionality of the deformation or condensate, as a free parameter and study the physics as a function of Δ . All the

fluctuations of the gravity backgrounds have positive mass squared, $M^2 > 0$, for all values considered, $0 < \Delta < 5$, in the physical portion of the parameter space, before the appearance of the phase transition. Interestingly, in portions of the parameter space well beyond the phase transition, the lightest scalar state in the theory becomes first an approximate dilaton, its mass being parametrically suppressed, and then a tachyon. All of these results confirm and generalize the findings in the three top-down models studied in Refs. [97–99], as well as the expectations of Refs. [92–94].

Restricting attention to the physical region of parameter space, in which the confining solutions are stable, we found some evidence that the mass of the lightest state in the spectrum becomes smaller in the limit $\Delta \rightarrow 5/2$ —half of the dimension of the space-time of the CFT that the dual theory flows from in the UV—in line with the suggestion, in Ref. [91], that such values of Δ are special. However, the lightest mass is light, but not parametrically so, as predicted in Ref. [94].

This study suggests that the phase transition we uncovered in this class of models cannot be rendered arbitrarily weak, nor of second order, and the lightest state cannot be a dilaton with tunable, small mass. The phenomena associated with confinement in the dual field theory and its specific implementation—which we borrowed from Witten’s model [73]—are playing an important role in yielding this conclusion. These findings support the arguments according to which inferring the properties of long-distance dynamics on the basis solely of the short-distance characterization of the theory (its fixed points and the classification of their deformations) is misleading, as the RG flow away from fixed points, ultimately leading to confinement, adds important nonperturbative effects.

It is premature to try to generalize these conclusions: the class of models analyzed here does not cover all possible realizations of confining field theories, and possibly the limitation of all these studies descends from the fact that confinement is described always in the same way, in terms of a shrinking circle in the internal geometry of a higher-dimensional gravity theory. For instance, top-down holographic models in which the analysis of the spectrum of fluctuations has been performed include Refs. [71,72,111], and the results (in particular, regarding the presence of light states) are model dependent, as the mechanism introducing a mass gap is different from the mechanism of interest here. We remind the reader that in Refs. [98,112] a similar model, but derived from maximal supergravity in seven dimensions, was studied. The main difference here is the fact that, in the bottom-up model considered in the present paper, Δ is a free parameter. The search for models that realize a weak phase transition, and in which a parametrically light dilaton can be realized, in the presence of a nearby instability in the parameter space of the theory, continues.

We conclude by anticipating that we will further extend this six-dimensional model, along lines similar to those followed in Ref. [112], in the complementary context of composite Higgs models, in future publications [113–115]. In this different context, we will extend the sigma model to incorporate an internal gauge symmetry. We will study how to break the corresponding global symmetry in the field theory, how to (weakly) gauge a subgroup, and how to exploit vacuum (mis)alignment to construct a composite Higgs model, with semirealistic features—in particular in reference to electroweak symmetry breaking.

All data displayed in the figures of this manuscript can be downloaded from Ref. [116]. We refer the reader to Refs. [117,118] and references therein for recent surveys on open science.

ACKNOWLEDGMENTS

We thank Ed Bennett for assisting in the preparation of the data release. The work of A. F. has been supported by the Science and Technology Facilities Council (STFC) Consolidated Grant No. ST/V507143/1. The work of M. P. has been supported in part by the STFC Consolidated Grants No. ST/P00055X/1 and No. ST/T000813/1. M. P. received funding from the European Research Council (ERC) under the European Union’s Horizon 2020 research and innovation program under Grant Agreement No. 813942.

APPENDIX A: SIGMA MODEL COUPLED TO GRAVITY

For the purpose of fixing our conventions, we write here the action of the two-derivative sigma model in D dimensions, consisting of n scalars Φ^a , with $a = 1, \dots, n$, coupled to gravity:

$$S = \int d^D x \sqrt{-g} \left[\frac{R}{4} - \frac{1}{2} g^{MN} G_{ab} \partial_M \Phi^a \partial_N \Phi^b - \mathcal{V}(\Phi^a) \right]. \quad (\text{A1})$$

We denote by $M = 0, \dots, 3, 5, \dots, D$ the D -dimensional space-time indexes. The D -dimensional metric g_{MN} has determinant g and signature mostly $+$. The D -dimensional Ricci scalar is denoted by R . The sigma-model metric is G_{ab} , and its inverse is G^{ab} . The potential \mathcal{V} is a function of the scalars Φ^a .

If we adopt the ansatz for the background solutions, that the metric is of the DW form and that the scalar fields only depend on the radial coordinate

$$ds_D^2 = dr^2 + e^{2A(r)} dx_{1,D-2}^2, \quad (\text{A2})$$

$$\Phi^a = \Phi^a(r), \quad (\text{A3})$$

then the equations of motion are given by

$$\partial_r^2 \Phi^a + (D-1) \partial_r A \partial_r \Phi^a + \mathcal{G}^a_{bc} \partial_r \Phi^b \partial_r \Phi^c - G^{ab} \frac{\partial \mathcal{V}}{\partial \Phi^b} = 0, \quad (\text{A4})$$

$$(D-1)(\partial_r A)^2 + \partial_r^2 A + \frac{4}{D-2} \mathcal{V} = 0, \quad (\text{A5})$$

$$(D-1)(D-2)(\partial_r A)^2 - 2G_{ab} \partial_r \Phi^a \partial_r \Phi^b + 4\mathcal{V} = 0, \quad (\text{A6})$$

where the sigma-model connection is

$$\mathcal{G}^d_{ab} \equiv \frac{1}{2} G^{dc} (\partial_a G_{cb} + \partial_b G_{ca} - \partial_c G_{ab}). \quad (\text{A7})$$

Furthermore, if one finds a solution, $\mathcal{W}(\Phi^a)$, to the following partial differential equation:

$$\mathcal{V} = \frac{1}{2} G^{ab} \frac{\partial \mathcal{V}}{\partial \Phi^a} \frac{\partial \mathcal{V}}{\partial \Phi^b} - \frac{D-1}{D-2} \mathcal{V}^2, \quad (\text{A8})$$

then any solution to the first-order equations

$$\partial_r A = -\frac{2}{D-2} \mathcal{W}, \quad (\text{A9})$$

$$\partial_r \Phi^a = G^{ab} \frac{\partial \mathcal{W}}{\partial \Phi^b} \quad (\text{A10})$$

is also a solution of the second-order classical equations (A4)–(A6).

1. Linearized equations for scalar fluctuations

In general, the linearized equations of motion can be put in gauge-invariant form following the formalism in Refs. [81–85] (where more details can be found). For the scalars, the gauge-invariant fluctuations \mathbf{a}^a obey the following equation:

$$[\mathcal{D}_r^2 + (D-1) \partial_r A \mathcal{D}_r - e^{-2A} q^2] \mathbf{a}^a - \mathcal{X}^a_c \mathbf{a}^c = 0. \quad (\text{A11})$$

Here, we used the notation that, given a field X^a , the sigma-model covariant and background-covariant derivatives are defined by $D_b X^a = \partial_b X^a + \mathcal{G}^a_{bc} X^c$ and $\mathcal{D}_r X^a = \partial_r X^a + \mathcal{G}^a_{bc} \partial_r \Phi^b X^c$, respectively, in terms of the sigma-model connection \mathcal{G}^a_{bc} of Eq. (A7). The sigma-model Riemann tensor is then given by $\mathcal{R}^a_{bcd} = \partial_c \mathcal{G}^a_{bd} - \partial_d \mathcal{G}^a_{bc} + \mathcal{G}^a_{ce} \mathcal{G}^e_{bd} - \mathcal{G}^a_{de} \mathcal{G}^e_{bc}$. The matrix \mathcal{X}^a_c reads as follows:

$$\begin{aligned} \mathcal{X}^a_c \equiv & -\mathcal{R}^a_{bcd} \partial_r \Phi^b \partial_r \Phi^d + D_c \left(G^{ab} \frac{\partial \mathcal{V}}{\partial \Phi^b} \right) \\ & + \frac{4}{(D-2) \partial_r A} \left[\partial_r \Phi^a \frac{\partial \mathcal{V}}{\partial \Phi^c} + G^{ab} \frac{\mathcal{V}}{\partial \Phi^b} \partial_r \Phi^d G_{dc} \right] \\ & + \frac{16\mathcal{V}}{(D-2)^2 (\partial_r A)^2} \partial_r \Phi^a \partial_r \Phi^b G_{bc}. \end{aligned} \quad (\text{A12})$$

We add infinitely large, boundary-localized mass terms for all the fluctuations of Φ^a , that hence satisfy Dirichlet

boundary conditions. The resulting boundary conditions for the gauge-invariant variables α^a are the following:

$$\begin{aligned} & \partial_r \Phi^c \partial_r \Phi^d G_{db} \mathcal{D}_\rho \alpha^b |_{r_i} \\ & = \left[\frac{(D-2) \partial_r A}{2} e^{-2A} q^2 \delta_b^c \right. \\ & \quad \left. + \partial_r \Phi^c \left(\frac{4\mathcal{V}}{(D-2) \partial_r A} \partial_r \Phi^d G_{db} + \frac{\partial \mathcal{V}}{\partial \Phi^b} \right) \right] \alpha^b |_{r_i}. \end{aligned} \quad (\text{A13})$$

APPENDIX B: OF SUPERPOTENTIALS

The associated superpotential, Eq. (6), that is used for example in the context of holographic renormalization when $\Delta > 5/2$, is not known in closed form. Yet, we can write it as a power expansion in ϕ , and we find that

$$\begin{aligned} \bar{\mathcal{W}}_6 = & -2 - \frac{1}{2} (5 - \Delta) \phi^2 - \frac{25(2\Delta - 5)}{16(4\Delta - 15)} \phi^4 - \frac{125(2\Delta - 5)(4\Delta^2 - 15\Delta + 25)}{64(4\Delta - 15)^2(6\Delta - 25)} \phi^6 \\ & - \frac{625(128\Delta^5 - 480\Delta^4 + 800\Delta^3 - 4 \times 10^3 \Delta^2 + 11250\Delta - 9375)}{1024(4\Delta - 15)^3(48\Delta^2 - 410\Delta + 875)} \phi^8 \\ & - \frac{625}{4096(25 - 6\Delta)^2(15 - 4\Delta)^4(16\Delta^2 - 142\Delta + 315)} (3072\Delta^8 + 25600\Delta^7 - 433600\Delta^6 \\ & + 1292 \times 10^3 \Delta^5 + 1065 \times 10^3 \Delta^4 - 10862500\Delta^3 + 18531250\Delta^2 - 12734375\Delta + 3515625) \phi^{10} \\ & - \frac{3125}{32768(25 - 6\Delta)^2(4\Delta - 15)^5(192\Delta^3 - 2584\Delta^2 + 11590\Delta - 17325)} (24576\Delta^{10} + 1320960\Delta^9 \\ & - 8153600\Delta^8 - 45968 \times 10^3 \Delta^7 + 473 \times 10^6 \Delta^6 - 12998 \times 10^5 \Delta^5 + 100425 \times 10^4 \Delta^4 \\ & + 133625 \times 10^4 \Delta^3 - 25625 \times 10^5 \Delta^2 + 10^9 \Delta + 87890625) \phi^{12} \\ & - \frac{15625}{131072(35 - 8\Delta)^2(15 - 4\Delta)^6(6\Delta - 25)^3(336\Delta^3 - 4612\Delta^2 + 21100\Delta - 32175)} (4718592\Delta^{14} \\ & + 714670080\Delta^{13} - 2224128 \times 10^3 \Delta^{12} - 140363776 \times 10^3 \Delta^{11} + 155181568 \times 10^4 \Delta^{10} - 54067432 \times 10^5 \Delta^9 \\ & - 6193644 \times 10^6 \Delta^8 + 107537295 \times 10^6 \Delta^7 - 3559741875 \times 10^5 \Delta^6 + 53236421875 \times 10^4 \Delta^5 \\ & - 2431853125 \times 10^5 \Delta^4 - 318709765625 \times 10^3 \Delta^3 + 450370605468750\Delta^2 \\ & - 162176513671875\Delta + 823974609375) \phi^{14} \\ & - \frac{78125}{4194304(35 - 8\Delta)^2(4\Delta - 15)^7(6\Delta - 25)^3(5376\Delta^4 - 98992\Delta^3 + 683500\Delta^2 - 2097300\Delta + 2413125)} \\ & \times (150994944\Delta^{16} + 57881395200\Delta^{15} + 1092472012800\Delta^{14} \\ & - 27151204352 \times 10^3 \Delta^{13} + 8460660736 \times 10^4 \Delta^{12} + 13597392384 \times 10^5 \Delta^{11} \\ & - 13484257056 \times 10^6 \Delta^{10} + 4795751472 \times 10^7 \Delta^9 - 398284926 \times 10^8 \Delta^8 \\ & - 254111197 \times 10^9 \Delta^7 + 9657946325 \times 10^8 \Delta^6 - 14713569328125 \times 10^5 \Delta^5 \\ & + 88646595703125 \times 10^4 \Delta^4 + 26974482421875 \times 10^4 \Delta^3 - 617424755859375 \times 10^3 \Delta^2 \\ & + 224028259277343750\Delta + 61798095703125) \phi^{16} \end{aligned}$$

$$\begin{aligned}
& -390625[16777216(25-6\Delta)^4(15-4\Delta)^8(16\Delta^2-142\Delta+315)^2 \\
& \times(48384\Delta^4-901680\Delta^3+6301100\Delta^2-19569500\Delta+22790625)]^{-1} \\
& \times(7247757312\Delta^{20}+6263874256896\Delta^{19}+303911927808\times 10^3\Delta^{18} \\
& -5902748929228800\Delta^{17}-2758035111936\times 10^4\Delta^{16}+13174340632576\times 10^5\Delta^{15} \\
& -115787186756608\times 10^5\Delta^{14}+31365013166976\times 10^6\Delta^{13}+17161524832384\times 10^7\Delta^{12} \\
& -18328634352128\times 10^8\Delta^{11}+726376592369\times 10^{10}\Delta^{10}-140457265478675\times 10^8\Delta^9 \\
& +3591879533675\times 10^9\Delta^8+4946038879446875\times 10^7\Delta^7-126333638659140625\times 10^6\Delta^6 \\
& +1469488973640625\times 10^8\Delta^5-7281017740966796875\times 10^4\Delta^4-14333258841552734375\times 10^3\Delta^3 \\
& +322610068359375\times 10^8\Delta^2-10350940532684326171875\Delta+115871429443359375)\phi^{18} \\
& -390625[134217728(25-6\Delta)^4(9-2\Delta)^2(4\Delta-15)^9(8\Delta-35)^3\times \\
& \times(193536\Delta^5-4526016\Delta^4+42336320\Delta^3-197998900\Delta^2+462983\times 10^3\Delta-433021875)]^{-1} \\
& \times(463856467968\Delta^{23}+870020787732480\Delta^{22}+93468471475568640\Delta^{21} \\
& -537522325998796800\Delta^{20}-4220626598363136\times 10^4\Delta^{19}+70461689518882816\times 10^4\Delta^{18} \\
& -24426057346514944\times 10^5\Delta^{17}-38568233605083136\times 10^6\Delta^{16} \\
& +51863822701075456\times 10^7\Delta^{15}-27603786074733376\times 10^8\Delta^{14} \\
& +5554033898884608\times 10^9\Delta^{13}+1756207389007328\times 10^{10}\Delta^{12} \\
& -1601187067059638\times 10^{11}\Delta^{11}+53057037376123675\times 10^{10}\Delta^{10} \\
& -922419869075040625\times 10^9\Delta^9+5120596044251203125\times 10^8\Delta^8 \\
& +138753717\times 10^3403125\times 10^{10}\Delta^7-371419078250947265625\times 10^7\Delta^6 \\
& +4075653348253369140625\times 10^6\Delta^5-20041289228924560546875\times 10^5\Delta^4 \\
& -9840867372802734375\times 10^7\Delta^3+54259196491241455078125\times 10^4\Delta^2 \\
& -169888076331138610839843750\Delta-60832500457763671875)\phi^{20}+\dots.
\end{aligned} \tag{B1}$$

We show explicitly terms up to $\mathcal{O}(\phi^{20})$ in order to allow the reader to inspect the presence of a pathology in the expansion: for special choices such as $\Delta = \frac{15}{4}, \frac{25}{6}, \frac{35}{8}, \frac{9}{2}, \frac{55}{12}, \frac{65}{14}, \frac{75}{16}, \frac{85}{18}, \frac{19}{4}, \dots$, some coefficients diverge.

APPENDIX C: ASYMPTOTIC EXPANSION OF THE BACKGROUND SOLUTIONS

In the main body of the paper, we showed the IR expansion for the confining solutions for any value of Δ , in Eqs. (28)–(30). For the singular domain-wall

solutions, we provided the IR expansions in Eqs. (42) and (43). Contrary to the IR expansions, the functional form of the UV expansions depends explicitly on Δ . In the main body of the paper, we reported the expansion for $\Delta = 3$. In this appendix, we provide a few additional representative examples of the UV expansions, expressed as power series in $z = e^{-\rho}$. For simplicity, we set $A_U = 0 = \chi_U$.

For $\Delta = 1/2$, and hence $\Delta_J = 1/2$, $\Delta_V = 9/2$, we have

$$\phi = z^{1/2}\phi_J + z^{9/2}\phi_V + \frac{3}{5}z^{11/2}\phi_J^2\phi_V + \frac{35}{192}z^{13/2}\phi_J^4\phi_V + o(z^7), \tag{C1}$$

$$\chi = -\frac{\log(z)}{3} - \frac{z\phi_J^2}{24} + z^5\left(\chi^5 - \frac{3\phi_J\phi_V}{100}\right) + z^6\left(\frac{25\chi^5\phi_J^2}{48} - \frac{11}{720}\phi_J^3\phi_V\right) + z^7\left(\frac{125\chi^5\phi_J^4}{896} - \frac{65\phi_J^5\phi_V}{16128}\right) + o(z^7), \tag{C2}$$

$$A = -\frac{4\log(z)}{3} - \frac{z\phi_J^2}{6} + z^5\left(\frac{\chi^5}{4} - \frac{3\phi_J\phi_V}{25}\right) + z^6\left(\frac{25\chi^5\phi_J^2}{192} - \frac{11}{180}\phi_J^3\phi_V\right) + z^7\left(\frac{125\chi^5\phi_J^4}{3584} - \frac{65\phi_J^5\phi_V}{4032}\right) + o(z^7). \tag{C3}$$

For $\Delta = 1$, and hence $\Delta_J = 1$, $\Delta_V = 4$, we have

$$\phi = z\phi_J + z^4\phi_V + \frac{21}{40}z^6\phi_J^2\phi_V + o(z^7), \quad (\text{C4})$$

$$\chi = -\frac{\log(z)}{3} - \frac{1}{24}z^2\phi_J^2 + \frac{1}{75}z^5(75\chi_5 - 4\phi_J\phi_V) - \frac{1}{280}z^7\phi_J^2(6\phi_J\phi_V - 125\chi_5) + o(z^7), \quad (\text{C5})$$

$$A = -\frac{4\log(z)}{3} - \frac{1}{6}z^2\phi_J^2 + \frac{1}{300}z^5(75\chi_5 - 64\phi_J\phi_V) + \frac{z^7(125\chi_5\phi_J^2 - 96\phi_J^3\phi_V)}{1120} + o(z^7). \quad (\text{C6})$$

For $\Delta = 3/2$, and hence $\Delta_J = 3/2$, $\Delta_V = 7/2$, we have

$$\phi = z^{3/2}\phi_J + z^{7/2}\phi_V + \frac{2}{5}z^{13/2}\phi_J^2\phi_V + o(z^7), \quad (\text{C7})$$

$$\chi = -\frac{\log(z)}{3} - \frac{1}{24}z^3\phi_J^2 + \frac{1}{100}z^5(100\chi_5 - 7\phi_J\phi_V) - \frac{1}{24}z^7\phi_V^2 + o(z^7), \quad (\text{C8})$$

$$A = -\frac{4\log(z)}{3} - \frac{1}{6}z^3\phi_J^2 + \frac{1}{100}z^5(25\chi_5 - 28\phi_J\phi_V) - \frac{1}{6}z^7\phi_V^2 + o(z^7). \quad (\text{C9})$$

For $\Delta = 17/10$, and hence $\Delta_J = 17/10$, $\Delta_V = 33/10$, we have

$$\phi = z^{17/10}\phi_J + z^{33/10}\phi_V + \frac{42}{125}z^{67/10}\phi_J^2\phi_V + o(z^7), \quad (\text{C10})$$

$$\chi = -\frac{\log(z)}{3} - \frac{1}{24}z^{17/5}\phi_J^2 + z^5\left(\chi_5 - \frac{187\phi_J\phi_V}{2500}\right) - \frac{1}{24}z^{33/5}\phi_V^2 + o(z^7), \quad (\text{C11})$$

$$A = -\frac{4\log(z)}{3} - \frac{1}{6}z^{17/5}\phi_J^2 + z^5\left(\frac{\chi_5}{4} - \frac{187\phi_J\phi_V}{625}\right) - \frac{1}{6}z^{33/5}\phi_V^2 + o(z^7). \quad (\text{C12})$$

For $\Delta = 7/4$, and hence $\Delta_J = 7/4$, $\Delta_V = 13/4$, we have

$$\phi = z^{7/4}\phi_J + z^{13/4}\phi_V + \frac{51}{160}z^{27/4}\phi_J^2\phi_V + o(z^7), \quad (\text{C13})$$

$$\chi = -\frac{\log(z)}{3} - \frac{1}{24}z^{7/2}\phi_J^2 + z^5\left(\chi_5 - \frac{91\phi_J\phi_V}{1200}\right) - \frac{1}{24}z^{13/2}\phi_V^2 + o(z^7), \quad (\text{C14})$$

$$A = -\frac{4\log(z)}{3} - \frac{1}{6}z^{7/2}\phi_J^2 + z^5\left(\frac{\chi_5}{4} - \frac{91\phi_J\phi_V}{300}\right) - \frac{1}{6}z^{13/2}\phi_V^2 + o(z^7). \quad (\text{C15})$$

For $\Delta = 9/5$, and hence $\Delta_J = 9/5$, $\Delta_V = 16/5$, we have

$$\phi = z^{9/5}\phi_J + z^{16/5}\phi_V + \frac{301z^{34/5}\phi_J^2\phi_V}{1000} + o(z^7), \quad (\text{C16})$$

$$\chi = -\frac{\log(z)}{3} - \frac{1}{24}z^{18/5}\phi_J^2 + z^5\left(\chi_5 - \frac{48\phi_J\phi_V}{625}\right) - \frac{1}{24}z^{32/5}\phi_V^2 + o(z^7), \quad (\text{C17})$$

$$A = -\frac{4\log(z)}{3} - \frac{1}{6}z^{18/5}\phi_J^2 + z^5\left(\frac{\chi_5}{4} - \frac{192\phi_J\phi_V}{625}\right) - \frac{1}{6}z^{32/5}\phi_V^2 + o(z^7). \quad (\text{C18})$$

For $\Delta = 37/20$, and hence $\Delta_J = 37/20$, $\Delta_V = 63/20$, we have

$$\phi = z^{37/20}\phi_J + z^{63/20}\phi_V + \frac{1131z^{137/20}\phi_J^2\phi_V}{4000} + o(z^7), \quad (\text{C19})$$

$$\chi = -\frac{\log(z)}{3} - \frac{1}{24}z^{37/10}\phi_J^2 + z^5\left(\chi_5 - \frac{777\phi_J\phi_V}{10000}\right) - \frac{1}{24}z^{63/10}\phi_V^2 + o(z^7), \quad (\text{C20})$$

$$A = -\frac{4\log(z)}{3} - \frac{1}{6}z^{37/10}\phi_J^2 + z^5\left(\frac{\chi_5}{4} - \frac{777\phi_J\phi_V}{2500}\right) - \frac{1}{6}z^{63/10}\phi_V^2 + o(z^7). \quad (\text{C21})$$

For $\Delta = 19/10$, and hence $\Delta_J = 19/10$, $\Delta_V = 31/10$, we have

$$\phi = z^{19/10}\phi_J + z^{31/10}\phi_V + \frac{33}{125}z^{69/10}\phi_J^2\phi_V + o(z^7), \quad (\text{C22})$$

$$\chi = -\frac{\log(z)}{3} - \frac{1}{24}z^{19/5}\phi_J^2 + z^5\left(\chi_5 - \frac{589\phi_J\phi_V}{7500}\right) - \frac{1}{24}z^{31/5}\phi_V^2 + o(z^7), \quad (\text{C23})$$

$$A = -\frac{4\log(z)}{3} - \frac{1}{6}z^{19/5}\phi_J^2 + z^5\left(\frac{\chi_5}{4} - \frac{589\phi_J\phi_V}{1875}\right) - \frac{1}{6}z^{31/5}\phi_V^2 + o(z^7). \quad (\text{C24})$$

For $\Delta = 39/20$, and hence $\Delta_J = 39/20$, $\Delta_V = 61/20$, we have

$$\phi = z^{39/20}\phi_J + z^{61/20}\phi_V + \frac{979z^{139/20}\phi_J^2\phi_V}{4000} + o(z^7), \quad (\text{C25})$$

$$\chi = -\frac{\log(z)}{3} - \frac{1}{24}z^{39/10}\phi_J^2 + z^5\left(\chi_5 - \frac{793\phi_J\phi_V}{10000}\right) - \frac{1}{24}z^{61/10}\phi_V^2 + o(z^7), \quad (\text{C26})$$

$$A = -\frac{4\log(z)}{3} - \frac{1}{6}z^{39/10}\phi_J^2 + z^5\left(\frac{\chi_5}{4} - \frac{793\phi_J\phi_V}{2500}\right) - \frac{1}{6}z^{61/10}\phi_V^2 + o(z^7). \quad (\text{C27})$$

For $\Delta = 2$, and hence $\Delta_J = 2$, $\Delta_V = 3$, we have

$$\phi = z^2\phi_J + z^3\phi_{\Delta_V} + \frac{9}{40}z^7\phi_J^2\phi_V + o(z^7), \quad (\text{C28})$$

$$\chi = -\frac{\log(z)}{3} - \frac{1}{24}z^4\phi_J^2 + \frac{1}{25}z^5(25\chi_5 - 2\phi_J\phi_V) - \frac{1}{24}z^6\phi_V^2 + o(z^7), \quad (\text{C29})$$

$$A = -\frac{4\log(z)}{3} - \frac{1}{6}z^4\phi_J^2 + \frac{1}{100}z^5(25\chi_5 - 32\phi_J\phi_V) - \frac{1}{6}z^6\phi_V^2 + o(z^7). \quad (\text{C30})$$

For $\Delta = 9/4$, and hence $\Delta_J = 9/4$, $\Delta_V = 11/4$, we have

$$\phi = z^{9/4}\phi_J + z^{11/4}\phi_V + o(z^7), \quad (\text{C31})$$

$$\chi = -\frac{\log(z)}{3} - \frac{1}{24}z^{9/2}\phi_J^2 + \frac{1}{400}z^5(400\chi_5 - 33\phi_J\phi_V) - \frac{1}{24}z^{11/2}\phi_V^2 + o(z^7), \quad (\text{C32})$$

$$A = -\frac{4\log(z)}{3} - \frac{1}{6}z^{9/2}\phi_J^2 + \frac{1}{100}z^5(25\chi_5 - 33\phi_J\phi_V) - \frac{1}{6}z^{11/2}\phi_V^2 + o(z^7). \quad (\text{C33})$$

For $\Delta = 23/10$, and hence $\Delta_J = 23/10$, $\Delta_V = 27/10$, we have

$$\phi = z^{23/10}\phi_J + z^{27/10}\phi_V + o(z^7), \quad (\text{C34})$$

$$\chi = -\frac{\log(z)}{3} - \frac{1}{24}z^{23/5}\phi_J^2 + \frac{z^5(2500\chi_5 - 207\phi_J\phi_V)}{2500} - \frac{1}{24}z^{27/5}\phi_V^2 + o(z^7), \quad (\text{C35})$$

$$A = -\frac{4\log(z)}{3} - \frac{1}{6}z^{23/5}\phi_J^2 + \frac{z^5(625\chi_5 - 828\phi_J\phi_V)}{2500} - \frac{1}{6}z^{27/5}\phi_V^2 + o(z^7). \quad (\text{C36})$$

For $\Delta = 47/20$, and hence $\Delta_J = 47/20$, $\Delta_V = 53/20$, we have

$$\phi = z^{47/20}\phi_J + z^{53/20}\phi_V + o(z^7), \quad (\text{C37})$$

$$\chi = -\frac{\log(z)}{3} - \frac{1}{24}z^{47/10}\phi_J^2 + \frac{z^5(30000\chi_5 - 2491\phi_J\phi_V)}{30000} - \frac{1}{24}z^{53/10}\phi_V^2 + o(z^7), \quad (\text{C38})$$

$$A = -\frac{4\log(z)}{3} - \frac{1}{6}z^{47/10}\phi_J^2 + \frac{z^5(1875\chi_5 - 2491\phi_J\phi_V)}{7500} - \frac{1}{6}z^{53/10}\phi_V^2 + o(z^7). \quad (\text{C39})$$

For $\Delta = 12/5$, and hence $\Delta_J = 12/5$, $\Delta_V = 13/5$, we have

$$\phi = z^{12/5}\phi_J + z^{13/5}\phi_V + o(z^7), \quad (\text{C40})$$

$$\chi = -\frac{\log(z)}{3} - \frac{1}{24}z^{24/5}\phi_J^2 + \frac{1}{625}z^5(625\chi_5 - 52\phi_J\phi_V) - \frac{1}{24}z^{26/5}\phi_V^2 + o(z^7), \quad (\text{C41})$$

$$A = -\frac{4\log(z)}{3} - \frac{1}{6}z^{24/5}\phi_J^2 + \frac{z^5(625\chi_5 - 832\phi_J\phi_V)}{2500} - \frac{1}{6}z^{26/5}\phi_V^2 + o(z^7). \quad (\text{C42})$$

For $\Delta = 49/20$, and hence $\Delta_J = 49/20$, $\Delta_V = 51/20$, we have

$$\phi = z^{49/20}\phi_J + z^{51/20}\phi_V + o(z^7), \quad (\text{C43})$$

$$\chi = -\frac{\log(z)}{3} - \frac{1}{24}z^{49/10}\phi_J^2 + \frac{z^5(10000\chi_5 - 833\phi_J\phi_V)}{10000} - \frac{1}{24}z^{51/10}\phi_V^2 + o(z^7), \quad (\text{C44})$$

$$A = -\frac{4\log(z)}{3} - \frac{1}{6}z^{49/10}\phi_J^2 + \frac{z^5(625\chi_5 - 833\phi_J\phi_V)}{2500} - \frac{1}{6}z^{51/10}\phi_V^2 + o(z^7). \quad (\text{C45})$$

For $\Delta = 249/100$, and hence $\Delta_J = 249/100$, $\Delta_V = 251/100$, we have

$$\phi = z^{249/100}\phi_J + z^{251/100}\phi_V + o(z^7), \quad (\text{C46})$$

$$\chi = -\frac{\log(z)}{3} - \frac{1}{24}z^{249/50}\phi_J^2 + z^5\left(\chi_5 - \frac{20833\phi_J\phi_V}{250000}\right) - \frac{1}{24}z^{251/50}\phi_V^2 + o(z^7), \quad (\text{C47})$$

$$A = -\frac{4\log(z)}{3} - \frac{1}{6}z^{249/50}\phi_J^2 + z^5\left(\frac{\chi_5}{4} - \frac{20833\phi_J\phi_V}{62500}\right) - \frac{1}{6}z^{251/50}\phi_V^2 + o(z^7). \quad (\text{C48})$$

For $\Delta = 2499/1000$, and hence $\Delta_J = 2499/1000$, $\Delta_V = 2501/1000$, we have

$$\phi = z^{2499/1000}\phi_J + z^{2501/1000}\phi_V + o(z^7), \quad (\text{C49})$$

$$\chi = -\frac{\log(z)}{3} - \frac{1}{24} z^{2499/500} \phi_J^2 + z^5 \left(\chi_5 - \frac{2083333 \phi_J \phi_V}{25000000} \right) - \frac{1}{24} z^{2501/500} \phi_V^2 + o(z^7), \quad (\text{C50})$$

$$A = -\frac{4 \log(z)}{3} - \frac{1}{6} z^{2499/500} \phi_J^2 + z^5 \left(\frac{\chi_5}{4} - \frac{2083333 \phi_J \phi_V}{6250000} \right) - \frac{1}{6} z^{2501/500} \phi_V^2 + o(z^7). \quad (\text{C51})$$

For $\Delta = 5/2$, and hence $\Delta_J = \Delta_V = 5/2$, we have

$$\begin{aligned} \phi &= \phi_V z^{5/2} + \phi_J z^{5/2} \log(z) + \frac{1}{200} (50 \phi_V^2 \phi_J - 25 \phi_V \phi_J^2 + 8 \phi_J^3) z^{15/2} \\ &\quad + \frac{1}{8} (4 \phi_V \phi_J^2 - \phi_J^3) z^{15/2} \log(z) + \frac{1}{4} \phi_J^3 z^{15/2} \log^2(z) + o(z^8), \end{aligned} \quad (\text{C52})$$

$$\chi = -\frac{\log(z)}{3} + \left(\chi_5 + \frac{1}{600} (-25 \phi_V^2 - 2 \phi_J^2) \right) z^5 - \frac{1}{12} \phi_V \phi_J z^5 \log(z) - \frac{1}{24} \phi_J^2 z^5 \log^2(z) + o(z^8), \quad (\text{C53})$$

$$A = -\frac{4 \log(z)}{3} + \frac{1}{300} (75 \chi_5 - 50 \phi_V^2 - 4 \phi_J^2) z^5 - \frac{1}{3} \phi_V \phi_J z^5 \log(z) - \frac{1}{6} \phi_J^2 z^5 \log^2(z) + o(z^8). \quad (\text{C54})$$

For $\Delta = 2501/1000$, and hence $\Delta_J = 2499/1000$, $\Delta_V = 2501/1000$, we have

$$\phi = z^{2499/1000} \phi_J + z^{2501/1000} \phi_V + o(z^7), \quad (\text{C55})$$

$$\chi = -\frac{\log(z)}{3} - \frac{1}{24} z^{2499/500} \phi_J^2 + z^5 \left(\chi_5 - \frac{2083333 \phi_J \phi_V}{25000000} \right) - \frac{1}{24} z^{2501/500} \phi_V^2 + o(z^7), \quad (\text{C56})$$

$$A = -\frac{4 \log(z)}{3} - \frac{1}{6} z^{2499/500} \phi_J^2 + z^5 \left(\frac{\chi_5}{4} - \frac{2083333 \phi_J \phi_V}{6250000} \right) - \frac{1}{6} z^{2501/500} \phi_V^2 + o(z^7). \quad (\text{C57})$$

For $\Delta = 251/100$, and hence $\Delta_J = 249/100$, $\Delta_V = 251/100$, we have

$$\phi = z^{249/100} \phi_J + z^{251/100} \phi_V + o(z^7), \quad (\text{C58})$$

$$\chi = -\frac{\log(z)}{3} - \frac{1}{24} z^{249/50} \phi_J^2 + z^5 \left(\chi_5 - \frac{20833 \phi_J \phi_V}{250000} \right) - \frac{1}{24} z^{251/50} \phi_V^2 + o(z^7), \quad (\text{C59})$$

$$A = -\frac{4 \log(z)}{3} - \frac{1}{6} z^{249/50} \phi_J^2 + z^5 \left(\frac{\chi_5}{4} - \frac{20833 \phi_J \phi_V}{62500} \right) - \frac{1}{6} z^{251/50} \phi_V^2 + o(z^7). \quad (\text{C60})$$

For $\Delta = 51/20$, and hence $\Delta_J = 49/20$, $\Delta_V = 51/20$, we have

$$\phi = z^{49/20} \phi_J + z^{51/20} \phi_V + o(z^7), \quad (\text{C61})$$

$$\chi = -\frac{\log(z)}{3} - \frac{1}{24} z^{49/10} \phi_J^2 + \frac{z^5 (10000 \chi_5 - 833 \phi_J \phi_V)}{10000} - \frac{1}{24} z^{51/10} \phi_V^2 + o(z^7), \quad (\text{C62})$$

$$A = -\frac{4 \log(z)}{3} - \frac{1}{6} z^{49/10} \phi_J^2 + \frac{z^5 (625 \chi_5 - 833 \phi_J \phi_V)}{2500} - \frac{1}{6} z^{51/10} \phi_V^2 + o(z^7). \quad (\text{C63})$$

For $\Delta = 13/5$, and hence $\Delta_J = 12/5$, $\Delta_V = 13/5$, we have

$$\phi = z^{12/5} \phi_J + z^{13/5} \phi_V + o(z^7), \quad (\text{C64})$$

$$\chi = -\frac{\log(z)}{3} - \frac{1}{24} z^{24/5} \phi_J^2 + \frac{1}{625} z^5 (625\chi_5 - 52\phi_J\phi_V) - \frac{1}{24} z^{26/5} \phi_V^2 + o(z^7), \quad (\text{C65})$$

$$A = -\frac{4\log(z)}{3} - \frac{1}{6} z^{24/5} \phi_J^2 + \frac{z^5(625\chi_5 - 832\phi_J\phi_V)}{2500} - \frac{1}{6} z^{26/5} \phi_V^2 + o(z^7). \quad (\text{C66})$$

For $\Delta = 53/20$, and hence $\Delta_J = 47/20$, $\Delta_V = 53/20$, we have

$$\phi = z^{47/20} \phi_J + z^{53/20} \phi_V + o(z^7), \quad (\text{C67})$$

$$\chi = -\frac{\log(z)}{3} - \frac{1}{24} z^{47/10} \phi_J^2 + \frac{z^5(30000\chi_5 - 2491\phi_J\phi_V)}{30000} - \frac{1}{24} z^{53/10} \phi_V^2 + o(z^7), \quad (\text{C68})$$

$$A = -\frac{4\log(z)}{3} - \frac{1}{6} z^{47/10} \phi_J^2 + \frac{z^5(1875\chi_5 - 2491\phi_J\phi_V)}{7500} - \frac{1}{6} z^{53/10} \phi_V^2 + o(z^7). \quad (\text{C69})$$

For $\Delta = 27/10$, and hence $\Delta_J = 23/10$, $\Delta_V = 27/10$, we have

$$\phi = z^{23/10} \phi_J + z^{27/10} \phi_V - \frac{125}{966} z^{69/10} \phi_J^3 + o(z^7), \quad (\text{C70})$$

$$\chi = -\frac{\log(z)}{3} - \frac{1}{24} z^{23/5} \phi_J^2 + \frac{z^5(2500\chi_5 - 207\phi_J\phi_V)}{2500} - \frac{1}{24} z^{27/5} \phi_V^2 + o(z^7), \quad (\text{C71})$$

$$A = -\frac{4\log(z)}{3} - \frac{1}{6} z^{23/5} \phi_J^2 + \frac{z^5(625\chi_5 - 828\phi_J\phi_V)}{2500} - \frac{1}{6} z^{27/5} \phi_V^2 + o(z^7). \quad (\text{C72})$$

For $\Delta = 11/4$, and hence $\Delta_J = 9/4$, $\Delta_V = 11/4$, we have

$$\phi = z^{9/4} \phi_J + z^{11/4} \phi_V - \frac{25}{144} z^{27/4} \phi_J^3 + o(z^7), \quad (\text{C73})$$

$$\chi = -\frac{\log(z)}{3} - \frac{1}{24} z^{9/2} \phi_J^2 + \frac{1}{400} z^5 (400\chi_5 - 33\phi_J\phi_V) - \frac{1}{24} z^{11/2} \phi_V^2 + o(z^7), \quad (\text{C74})$$

$$A = -\frac{4\log(z)}{3} - \frac{1}{6} z^{9/2} \phi_J^2 + \frac{1}{100} z^5 (25\chi_5 - 33\phi_J\phi_V) - \frac{1}{6} z^{11/2} \phi_V^2 + o(z^7). \quad (\text{C75})$$

For $\Delta = 3$, and hence $\Delta_J = 2$, $\Delta_V = 3$, we have

$$\phi = z^2 \phi_J + z^3 \phi_V - \frac{25}{48} z^6 \phi_J^3 - \frac{57}{80} z^7 (\phi_J^2 \phi_V) + o(z^7), \quad (\text{C76})$$

$$\chi = -\frac{\log(z)}{3} - \frac{1}{24} z^4 \phi_J^2 + z^5 \left(\chi_5 - \frac{2\phi_J\phi_V}{25} \right) - \frac{1}{24} z^6 \phi_V^2 + o(z^7), \quad (\text{C77})$$

$$A = -\frac{4\log(z)}{3} - \frac{1}{6} z^4 \phi_J^2 + z^5 \left(\frac{\chi_5}{4} - \frac{8\phi_J\phi_V}{25} \right) - \frac{1}{6} z^6 \phi_V^2 + o(z^7). \quad (\text{C78})$$

For $\Delta = 7/2$, and hence $\Delta_J = 3/2$, $\Delta_V = 7/2$, we have

$$\phi = z^{3/2} \phi_J + z^{7/2} \phi_V - \frac{25}{6} z^{9/2} \phi_J^3 - \frac{21}{10} z^{13/2} \phi_J^2 \phi_V + o(z^7), \quad (\text{C79})$$

$$\chi = -\frac{\log(z)}{3} - \frac{1}{24} z^3 \phi_J^2 + \frac{1}{100} z^5 (100\chi_5 - 7\phi_J\phi_V) + \frac{25}{96} z^6 \phi_J^4 - \frac{1}{24} z^7 \phi_V^2 + o(z^7), \quad (\text{C80})$$

$$A = -\frac{4 \log(z)}{3} - \frac{1}{6} z^3 \phi_J^2 + \frac{1}{100} z^5 (25\chi_5 - 28\phi_J \phi_V) + \frac{25}{24} z^6 \phi_J^4 - \frac{1}{6} z^7 \phi_V^2 + o(z^7). \quad (\text{C81})$$

For $\Delta = 4$, and hence $\Delta_J = 1$, $\Delta_V = 4$, we have

$$\phi = z\phi_J + \frac{75}{8} z^3 \phi_J^3 + z^4 \phi_V - \frac{7875}{64} z^5 \phi_J^5 - \frac{51}{10} z^6 \phi_J^2 \phi_V + \frac{183125 z^7 \phi_J^7}{1536} + o(z^7), \quad (\text{C82})$$

$$\chi = -\frac{\log(z)}{3} - \frac{1}{24} z^2 \phi_J^2 - \frac{75}{128} z^4 \phi_J^4 + \frac{1}{75} z^5 (75\chi_5 - 4\phi_J \phi_V) + \frac{3125 z^6 \phi_J^6}{1536} + \frac{1}{280} z^7 (125\chi_5 \phi_J^2 - 156\phi_J^3 \phi_V) + o(z^7), \quad (\text{C83})$$

$$A = -\frac{4 \log(z)}{3} - \frac{1}{6} z^2 \phi_J^2 - \frac{75}{32} z^4 \phi_J^4 + \frac{1}{300} z^5 (75\chi_5 - 64\phi_J \phi_V) + \frac{3125}{384} z^6 \phi_J^6 + \frac{z^7 (125\chi_5 \phi_J^2 - 2496\phi_J^3 \phi_V)}{1120} + o(z^7). \quad (\text{C84})$$

For $\Delta = 24/5$, and hence $\Delta_J = 1/5$, $\Delta_V = 24/5$, we have

$$\begin{aligned} \phi = & z^{1/5} \phi_J + \frac{2875}{168} z^{3/5} \phi_J^3 + \frac{589375 z \phi_J^5}{1216} + \frac{1194097540625 z^{7/5} \phi_J^7}{72930816} + \frac{40083780796875 z^{9/5} \phi_J^9}{64827392} \\ & + \frac{206305363012094528125 z^{11/5} \phi_J^{11}}{8070232375296} + \frac{51555188135555851650546875 z^{13/5} \phi_J^{13}}{44741368288641024} \\ & + \frac{220895018700707881287319140625 z^{15/5} \phi_J^{15}}{3872162055526023168} + \frac{143635271586199611133308619908203125 z^{17/5} \phi_J^{17}}{45319784697876575158272} \\ & + \frac{2030227399573934911294696548892509765625 z^{19/5} \phi_J^{19}}{9789073494741340234186752} \\ & + \frac{62734499516892742142454970327066041783203125 z^{21/5} \phi_J^{21}}{3471858066134928669724901376} \\ & + \frac{703737750200907787167436115783648540622242333984375 z^{23/5} \phi_J^{23}}{202562087010576278306429645881344} \\ & + z^{24/5} \phi_V - \frac{42889968257354026233434739048798684916940287126220703125 z^{25/5} \phi_J^{25}}{10209129185330444266440541524197376} \\ & - \frac{5313}{125} z^{26/5} (\phi_J^2 \phi_V) + \frac{40372906759830069883219591463928127456136451751634521484375 z^{27/5} \phi_J^{27}}{5811221188951714835775331565278593024} \\ & + \frac{512647 z^{28/5} \phi_J^4 \phi_V}{3024} + \frac{23451902891374040266318476466845032509323071584144748101806640625 z^{29/5} \phi_J^{29}}{1344344664967333903248922102985288595800064} \\ & + \frac{2812375255 z^6 \phi_J^6 \phi_V}{6664896} - \frac{9356448978981275 z^{32/5} (\phi_J^8 \phi_V)}{786777643008} \\ & + \frac{3382994549224018067073083754105413390854841531398992869892655029296875 z^{31/5} \phi_J^{31}}{12873444511727189457511678058187123593381412864} \\ & + \frac{63252672595173277436174439987322783944040397901181003729679595947265625 z^{33/5} \phi_J^{33}}{11443061788201946184454824940610776527450144768} \\ & - \frac{882653673174311913125 z^{34/5} (\phi_J^{10} \phi_V)}{1090473813209088} + \mathcal{O}(z^7), \quad (\text{C85}) \end{aligned}$$

$$\begin{aligned}
\chi = & -\frac{\log(z)}{3} - \frac{1}{24}\phi_J^2 z^{2/5} - \frac{2875\phi_J^4 z^{4/5}}{2688} - \frac{445840625\phi_J^6 z^{6/5}}{12870144} - \frac{1245177090625\phi_J^8 z^{8/5}}{1000194048} \\
& - \frac{12757500935258125\phi_J^{10} z^2}{266051616768} - \frac{252462758077427834375\phi_J^{12} z^{12/5}}{129123718004736} \\
& - \frac{219400845248171582865859375\phi_J^{14} z^{14/5}}{2607782608823648256} - \frac{595634988671267098623623224609375\phi_J^{16} z^{16/5}}{155382118964148257685504} \\
& - \frac{37370923454539023891704902220703125\phi_J^{18} z^{18/5}}{199777010096762045595648} - \frac{3005589851661754675633072282749116796875\phi_J^{20} z^4}{299011699475735483516977152} \\
& - \frac{390603999209272169612305206890628037373755859375\phi_J^{22} z^{22/5}}{607686261031728834919288937644032} \\
& - \frac{1396398597179619157280207994845812226729262841796875\phi_J^{24} z^{24/5}}{19445960353015322717417246004609024} \\
& + \left(-\frac{1}{625}(8\phi_J\phi_V) + \chi_5 \right) z^5 + \frac{1306083301937461832252797063598660554434038579290771484375\phi_J^{26} z^{26/5}}{605197178106542873611459530155442044928} \\
& + \left(-\frac{4117\phi_J^3\phi_V}{70875} + \frac{125\phi_J^2\chi_5}{216} \right) z^{27/5} + \frac{5\phi_J^4(-9784936\phi_J\phi_V + 55981125\chi_5)z^{29/5}}{19994688} \\
& + \frac{13030865310005017933330153469549477844134773156086490478515625\phi_J^{28} z^{28/5}}{474474587635529612911384271641866563223552} \\
& + \frac{7032769665707387278806255307823137953470132552224159218505859375\phi_J^{30} z^6}{10754757319738671225991376823882308766400512} \\
& - \frac{25(\phi_J^6(2692663154104\phi_J\phi_V - 10082616060375\chi_5))z^{31/5}}{590083232256} \\
& + \frac{5540969477438023313564601832074044301054003663389867568262069091796875\phi_J^{32} z^{32/5}}{290788393676661220687322610255520909403438972928} \\
& - \frac{25(\phi_J^8(35613091214958616\phi_J\phi_V - 90309329147491875\chi_5))z^{33/5}}{155781973315584} \\
& + \frac{181830278970246170965622209207842711341265597685817924668243991119384765625\phi_J^{34} z^{34/5}}{294132460203942824725226820273459399861578521116672} \\
& + \mathcal{O}(z^7), \tag{C86}
\end{aligned}$$

$$\begin{aligned}
A = & -\frac{4\log(z)}{3} - \frac{1}{6}\phi_J^2 z^{2/5} - \frac{2875}{672}\phi_J^4 z^{4/5} - \frac{445840625\phi_J^6 z^{6/5}}{3217536} - \frac{1245177090625\phi_J^8 z^{8/5}}{250048512} \\
& - \frac{12757500935258125\phi_J^{10} z^2}{66512904192} - \frac{252462758077427834375\phi_J^{12} z^{12/5}}{32280929501184} \\
& - \frac{219400845248171582865859375\phi_J^{14} z^{14/5}}{651945652205912064} - \frac{595634988671267098623623224609375\phi_J^{16} z^{16/5}}{38845529741037064421376} \\
& - \frac{37370923454539023891704902220703125\phi_J^{18} z^{18/5}}{49944252524190511398912} - \frac{3005589851661754675633072282749116796875\phi_J^{20} z^4}{74752924868933870879244288} \\
& - \frac{390603999209272169612305206890628037373755859375\phi_J^{22} z^{22/5}}{151921565257932208729822234411008} \\
& - \frac{1396398597179619157280207994845812226729262841796875\phi_J^{24} z^{24/5}}{4861490088253830679354311501152256} \\
& + \left(-\frac{1}{625}(32\phi_J\phi_V) + \frac{\chi_5}{4} \right) z^5 + \frac{1306083301937461832252797063598660554434038579290771484375\phi_J^{26} z^{26/5}}{151299294526635718402864882538860511232}
\end{aligned}$$

$$\begin{aligned}
& + \left(-\frac{16468\phi_J^3\phi_V}{70875} + \frac{125\phi_J^2\chi_5}{864} \right) z^{27/5} + \left(-\frac{873655\phi_J^5\phi_V}{89262} + \frac{181875\phi_J^4\chi_5}{51968} \right) z^{29/5} \\
& + \frac{13030865310005017933330153469549477844134773156086490478515625\phi_J^{28}z^{28/5}}{118618646908882403227846067910466640805888} \\
& + \frac{7032769665707387278806255307823137953470132552224159218505859375\phi_J^{30}z^6}{2688689329934667806497844205970577191600128} \\
& + \frac{25\phi_J^6(-43082610465664\phi_J\phi_V + 10082616060375\chi_5)z^{31/5}}{2360332929024} \\
& + \frac{5540969477438023313564601832074044301054003663389867568262069091796875\phi_J^{32}z^{32/5}}{72697098419165305171830652563880227350859743232} \\
& - \frac{25(\phi_J^8(569809459439337856\phi_J\phi_V - 90309329147491875\chi_5))z^{33/5}}{623127893262336} \\
& + \frac{181830278970246170965622209207842711341265597685817924668243991119384765625\phi_J^{34}z^{34/5}}{73533115050985706181306705068364849965394630279168} + \mathcal{O}(z^7).
\end{aligned} \tag{C87}$$

APPENDIX D: ASYMPTOTIC EXPANSIONS OF THE FLUCTUATIONS

As described in the body of the paper, in order to improve the numerical convergence of the spectra of fluctuations, we write the asymptotic expansions of such solutions, both in the IR and in the UV. For the UV case, the expansion depends crucially on Δ ; while we did compute it explicitly for all the values of Δ used in the

numerical study, we report here only one example, for illustrative purposes.

1. IR expansions

For convenience, we put $\rho_o = 0$ and $A_I = 0$ in this subsection,² while $\chi_I = 0$ in order to avoid a conical singularity, as explained in the main text. For the fluctuations of the scalars $\Phi^a = \{\phi, \chi\}$, we have

$$\begin{aligned}
\mathbf{a}^1 &= \mathbf{a}_{I,0}^1 + \mathbf{a}_{I,I}^1 \log(\rho) + \frac{1}{4}\rho^2 \left[-\frac{1}{4}\Delta(\mathbf{a}_{I,0}^1(\Delta(15\phi_I^2 - 4) + 20) + 6\phi_I(\mathbf{a}_{I,0}^2 - \mathbf{a}_{I,I}^2)(\Delta(5\phi_I^2 - 4) + 20)) \right. \\
& + q^2(\mathbf{a}_{I,0}^1 - \mathbf{a}_{I,I}^1) - \frac{1}{48}\mathbf{a}_{I,I}^1(\Delta(25\Delta\phi_I^4 + 20(10 - 11\Delta)\phi_I^2 + 48(\Delta - 5)) + 400) \\
& \left. + \log(\rho) \left(\mathbf{a}_{I,I}^1 \left(-\frac{15\Delta^2\phi_I^2}{4} + (\Delta - 5)\Delta + q^2 \right) - \frac{3}{2}\mathbf{a}_{I,I}^2\Delta\phi_I(\Delta(5\phi_I^2 - 4) + 20) \right) \right] + \mathcal{O}(\rho^4), \tag{D1}
\end{aligned}$$

$$\begin{aligned}
\mathbf{a}^2 &= \mathbf{a}_{I,0}^2 + \mathbf{a}_{I,I}^2 \log(\rho) + \frac{1}{4}\rho^2 \left[-\frac{1}{4}\Delta\phi_I(\mathbf{a}_{I,0}^1 - \mathbf{a}_{I,I}^1)(\Delta(5\phi_I^2 - 4) + 20) + q^2(\mathbf{a}_{I,0}^2 - \mathbf{a}_{I,I}^2) \right. \\
& - \frac{3}{8}\mathbf{a}_{I,0}^2(\Delta\phi_I^2(\Delta(5\phi_I^2 - 8) + 40) + 80) + \frac{13}{48}\mathbf{a}_{I,I}^2(\Delta\phi_I^2(\Delta(5\phi_I^2 - 8) + 40) + 80) \\
& \left. + \log(\rho) \left(-\frac{5}{4}\mathbf{a}_{I,I}^1\Delta^2\phi_I^3 + \mathbf{a}_{I,I}^1(\Delta - 5)\Delta\phi_I + \mathbf{a}_{I,I}^2 \left(-\frac{15}{8}\Delta^2\phi_I^4 + 3(\Delta - 5)\Delta\phi_I^2 + q^2 - 30 \right) \right) \right] + \mathcal{O}(\rho^4). \tag{D2}
\end{aligned}$$

For the fluctuations of the vector χ_M , we have

$$\begin{aligned}
\mathbf{v} &= \mathbf{v}_{I,-2}\rho^{-2} + \frac{1}{2}q^2\mathbf{v}_{I,-2}\log(\rho) + \mathbf{v}_{I,0} + \frac{1}{12288}\rho^2[1536q^2\mathbf{v}_{I,0} + 80\Delta^2\mathbf{v}_{I,-2}\phi_I^4(2(8\Delta^2 - 50\Delta + 75) - 3q^2) \\
& + 128(\Delta - 5)\Delta\mathbf{v}_{I,-2}\phi_I^2(-3(\Delta - 5)\Delta + 3q^2 - 50) - 64(9q^4 + 60q^2 - 500)\mathbf{v}_{I,-2} + 125\Delta^4\mathbf{v}_{I,-2}\phi_I^8 \\
& - 1000(\Delta - 2)\Delta^3\mathbf{v}_{I,-2}\phi_I^6 + 768q^4\mathbf{v}_{I,-2}\log(\rho)] + \mathcal{O}(\rho^4). \tag{D3}
\end{aligned}$$

²The dependence on ρ_o and A_I can be reinstated by making the substitutions $\rho \rightarrow \rho - \rho_o$ and $q^2 \rightarrow e^{-2A_I}q^2$ in the expressions.

For the tensor fluctuations e_{ν}^{μ} , we have

$$e = e_{I,0} + e_{I,I} \log(\rho) + \frac{1}{192} \rho^2 [48q^2(e_{I,0} - e_{I,I}) - 25\Delta^2 e_{I,I} \phi_I^4 + 40(\Delta - 5)\Delta e_{I,I} \phi_I^2 - 400e_{I,I} + 48e_{I,I} q^2 \log(\rho)] + \mathcal{O}(\rho^4). \quad (\text{D4})$$

2. UV expansions

In this subsection, we put $\Delta = 3$, and $A_U = 0 = \chi_U$.³ We write the expansions in terms of $z \equiv e^{-\rho}$. For the fluctuations of the scalars, we have

$$\mathbf{a}^1 = \mathbf{a}_2^1 z^2 + \mathbf{a}_3^1 z^3 + \frac{1}{2} \mathbf{a}_2^1 q^2 z^4 + \frac{1}{6} \mathbf{a}_3^1 q^2 z^5 + \frac{1}{48} \mathbf{a}_2^1 (2q^4 - 99\phi_J^2) z^6 + \mathcal{O}(z^7), \quad (\text{D5})$$

$$\mathbf{a}^2 = \mathbf{a}_0^2 - \frac{1}{6} \mathbf{a}_0^2 q^2 z^2 + \frac{1}{24} \mathbf{a}_0^2 q^4 z^4 + \mathbf{a}_5^2 z^5 + \frac{1}{144} \mathbf{a}_0^2 q^2 (q^4 - 14\phi_J^2) z^6 + \mathcal{O}(z^7). \quad (\text{D6})$$

For the vector fluctuations, we have

$$\mathbf{v} = \mathbf{v}_0 - \frac{1}{6} q^2 \mathbf{v}_0 z^2 + \frac{1}{24} q^4 \mathbf{v}_0 z^4 + \mathbf{v}_5 z^5 + \frac{1}{144} q^2 \mathbf{v}_0 (q^4 - 14\phi_J^2) z^6 + \frac{1}{70} q^2 (70\mathbf{v}_0 \chi_5 - 2\mathbf{v}_0 \phi_J \phi_V + 5\mathbf{v}_5) z^7 + \mathcal{O}(z^8). \quad (\text{D7})$$

For the tensor fluctuations, we have

$$e = e_0 - \frac{1}{6} e_0 q^2 z^2 + \frac{1}{24} e_0 q^4 z^4 + e_5 z^5 + \mathcal{O}(z^6). \quad (\text{D8})$$

APPENDIX E: PROBE APPROXIMATION

In this appendix, we further discuss the probe approximation. More details can be found in Ref. [86]. The fluctuations $\mathbf{a}^a = \varphi^a - \frac{\partial_r \Phi^a}{6\partial_r A} h$ are formed by the mixing of the fluctuations of the scalars $\Phi^a = (\phi, \chi)$ and fluctuations h of the trace of the four-dimensional part of the metric. The latter couples to the trace of the stress-energy tensor of the boundary theory. If \mathbf{a}^a is mostly composed of h , and hence $\mathbf{a}^a \simeq \frac{\partial_r \Phi^a}{6\partial_r A} h$, the couplings of the states sourced by the operators at the boundary are well approximated by the dilatonic counterparts. Conversely, in the probe approximation for computing spectra, one neglects the mixing between the scalar and metric fluctuations. This will lead to correct results only if $\mathbf{a}^a \simeq \varphi^a$, such that the contribution of h in Eq. (A11) can be neglected.

The probe approximation is hence obtained by neglecting the contributions from the metric fluctuations, in particular h , in Eqs. (A11) and (A13), leading to [86]

$$0 = [\mathcal{D}_r^2 + (D-1)\partial_r A \mathcal{D}_r - e^{-2A} q^2] \mathbf{p}^a - [V^a|_c - \mathcal{R}^a{}_{bcd} \partial_r \Phi^b \partial_r \Phi^d] \mathbf{p}^c \quad (\text{E1})$$

for the equations of motion, while the boundary conditions reduce to

$$0 = \mathbf{p}^a|_{r_i}. \quad (\text{E2})$$

In these equations, we have replaced \mathbf{a}^a with the probe fluctuations that we denote by \mathbf{p}^a .

We perform the calculation of the spectra of scalar fluctuations in two ways for $\Delta = 5/2$ in the body of the paper. First, by solving the exact Eq. (A11), with the boundary conditions in Eq. (A13), and finding the spectrum of masses. Then, we repeat the calculation for the same background, but using the probe approximation and solving Eq. (E1), with the boundary conditions in Eq. (E2). If the two processes result in different spectra, overlap with the dilaton cannot be neglected. In the next subsections, IR and UV expansions for fluctuations in the probe approximation are given.

1. IR expansions

In this subsection, we put $\Delta = 5/2$. As in Appendix D, we put $\rho_o = 0$ and $A_I = 0$, while $\chi_I = 0$ in order to avoid a conical singularity. For the fluctuations of the scalars in the probe approximation, we have

³The dependence on χ_U and A_U can be reinstated by making the substitution $q^2 \rightarrow e^{2\chi_U - 2A_U} q^2$ in the expressions.

$$\begin{aligned}
\mathbf{p}^1 = & \mathbf{p}_{I,0}^1 + \mathbf{p}_{I,l}^1 \log(\rho) + \rho^2 \left[\Delta \left(-\frac{5\mathbf{p}_{I,l}^2 \phi_I}{2} + \frac{5\mathbf{p}_{I,0}^2 \phi_I}{2} \right) + \Delta^2 \left(\frac{\mathbf{p}_{I,l}^2 \phi_I}{2} - \frac{\mathbf{p}_{I,0}^2 \phi_I}{2} - \frac{5\mathbf{p}_{I,l}^2 \phi_I^3}{8} + \frac{5\mathbf{p}_{I,0}^2 \phi_I^3}{8} \right) \right. \\
& + \mathbf{p}_{I,0}^1 \left(\frac{q^2}{4} - \frac{5\Delta}{4} + \Delta^2 \left(\frac{1}{4} - \frac{15\phi_I^2}{16} \right) \right) + \mathbf{p}_{I,l}^1 \left(-\frac{25}{12} - \frac{q^2}{4} + \Delta \left(\frac{5}{4} - \frac{25\phi_I^2}{24} \right) + \Delta^2 \left(-\frac{1}{4} + \frac{55\phi_I^2}{48} - \frac{25\phi_I^4}{192} \right) \right) \\
& \left. + \left(\frac{5\mathbf{p}_{I,l}^2 \Delta \phi_I}{2} + \Delta^2 \left(-\frac{\mathbf{p}_{I,l}^2 \phi_I}{2} + \frac{5\mathbf{p}_{I,l}^2 \phi_I^3}{8} \right) + \mathbf{p}_{I,l}^1 \left(\frac{q^2}{4} - \frac{5\Delta}{4} + \Delta^2 \left(\frac{1}{4} - \frac{15\phi_I^2}{16} \right) \right) \right) \log(\rho) \right] + \mathcal{O}(\rho^4), \quad (\text{E3})
\end{aligned}$$

$$\begin{aligned}
\mathbf{p}^2 = & \mathbf{p}_{I,0}^2 + \mathbf{p}_{I,l}^2 \log(\rho) + \rho^2 \left[\Delta \left(-\frac{5\mathbf{p}_{I,l}^1 \phi_I}{12} + \frac{5\mathbf{p}_{I,0}^1 \phi_I}{12} \right) + \Delta^2 \left(\frac{\mathbf{p}_{I,l}^1 \phi_I}{12} - \frac{\mathbf{p}_{I,0}^1 \phi_I}{12} - \frac{5\mathbf{p}_{I,l}^1 \phi_I^3}{48} + \frac{5\mathbf{p}_{I,0}^1 \phi_I^3}{48} \right) \right. \\
& + \mathbf{p}_{I,l}^2 \left(-\frac{5}{4} - \frac{q^2}{4} - \frac{5\Delta \phi_I^2}{8} + \Delta^2 \left(\frac{\phi_I^2}{8} - \frac{5\phi_I^4}{64} \right) \right) + \mathbf{p}_{I,0}^2 \left(-\frac{5}{6} + \frac{q^2}{4} - \frac{5\Delta \phi_I^2}{12} + \Delta^2 \left(\frac{\phi_I^2}{12} - \frac{5\phi_I^4}{96} \right) \right) \\
& \left. + \left(\frac{5\mathbf{p}_{I,l}^1 \Delta \phi_I}{12} + \Delta^2 \left(-\frac{\mathbf{p}_{I,l}^1 \phi_I}{12} + \frac{5\mathbf{p}_{I,l}^1 \phi_I^3}{48} \right) + \mathbf{p}_{I,l}^2 \left(-\frac{5}{6} + \frac{q^2}{4} - \frac{5\Delta \phi_I^2}{12} + \Delta^2 \left(\frac{\phi_I^2}{12} - \frac{5\phi_I^4}{96} \right) \right) \right) \log(\rho) \right] + \mathcal{O}(\rho^4). \quad (\text{E4})
\end{aligned}$$

2. UV expansions

For the UV expansions we put $A_U = 0 = \chi_U$, as explained in Appendix D. Also, the expansions are considered for $\Delta = 5/2$ and are written in terms of $z \equiv e^{-\rho}$.

The fluctuations of the scalars in the probe approximation are more complicated to derive in this case as some of the exponents in expansions are nonrational numbers. The part of the expansion which is of importance in our calculations will be in the following form:

$$\mathbf{p}^1 = \log(z) z^{5/2} \mathbf{p}_{5/2,l}^1 (1 + \dots) + z^{5/2} \mathbf{p}_{5/2}^1 (1 + \dots), \quad (\text{E5})$$

$$\mathbf{p}^2 = z^{\alpha_-} \mathbf{p}_-^2 (1 + \dots) + z^{\alpha_+} \mathbf{p}_+^2 (1 + \dots), \quad (\text{E6})$$

where $\alpha_{\pm} \equiv (5 \pm \sqrt{35/3})/2$.

APPENDIX F: MORE ABOUT THE FREE ENERGY

In this short appendix, we report some details of the free energy density study for values of Δ close to $\Delta \simeq 1.8$. In Fig. 11 we show a detail of Fig. 8, that highlights the evolution of the free energy of the confining solutions. We notice that this is monotonic for $\Delta = 1.7$, while it has a local maximum and minimum, and changes in concavity, when $\Delta = 1.95$. It would be tempting to correlate this behavior with the appearance of a tachyon in the spectrum, but, as we comment in the main body of the paper, the presence of divergences, treated via holographic renormalization, turns the concavity of \mathcal{F} into a scheme-dependent quantity. We hence do not further pursue this line of enquiry in this paper.

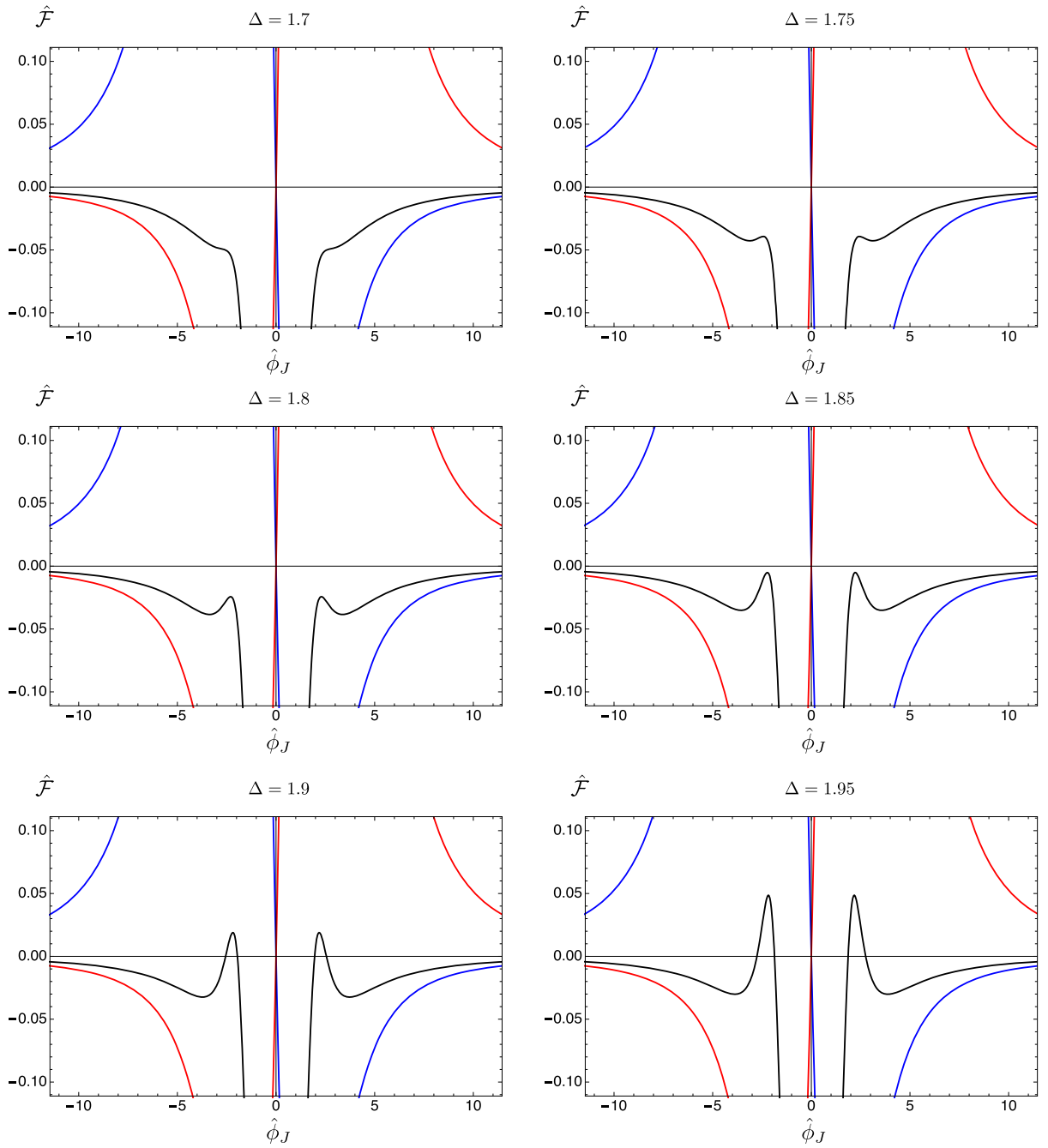


FIG. 11. The free energy $\hat{\mathcal{F}}$ as a function of the source $\hat{\phi}_J$, in units of the scale Λ , for representative choices of Δ near $\Delta \simeq 1.8$, above which the spectrum of fluctuations contains a tachyon in part of the parameter space. The black curve denotes the confining solutions, while the red and blue solutions are singular domain-wall ones.

[1] G. Aad *et al.* (ATLAS Collaboration), Observation of a new particle in the search for the Standard Model Higgs boson with the ATLAS detector at the LHC, *Phys. Lett. B* **716**, 1 (2012).

[2] S. Chatrchyan *et al.* (CMS Collaboration), Observation of a new boson at a mass of 125 GeV with the CMS experiment at the LHC, *Phys. Lett. B* **716**, 30 (2012).

- [3] W. D. Goldberger, B. Grinstein, and W. Skiba, Distinguishing the Higgs Boson from the Dilaton at the Large Hadron Collider, *Phys. Rev. Lett.* **100**, 111802 (2008).
- [4] A. A. Migdal and M. A. Shifman, Dilaton effective Lagrangian in gluodynamics, *Phys. Lett.* **114B**, 445 (1982).
- [5] S. Coleman, *Aspects of Symmetry: Selected Erice Lectures* (Cambridge University Press, Cambridge, England, 2010).
- [6] C. N. Leung, S. T. Love, and W. A. Bardeen, Spontaneous symmetry breaking in scale invariant quantum electrodynamics, *Nucl. Phys.* **B273**, 649 (1986).
- [7] W. A. Bardeen, C. N. Leung, and S. T. Love, The Dilaton and Chiral Symmetry Breaking, *Phys. Rev. Lett.* **56**, 1230 (1986).
- [8] K. Yamawaki, M. Bando, and K. i. Matumoto, Scale Invariant Technicolor Model and a Technidilaton, *Phys. Rev. Lett.* **56**, 1335 (1986).
- [9] D. K. Hong, S. D. H. Hsu, and F. Sannino, Composite Higgs from higher representations, *Phys. Lett. B* **597**, 89 (2004).
- [10] D. D. Dietrich, F. Sannino, and K. Tuominen, Light composite Higgs from higher representations versus electroweak precision measurements: Predictions for CERN LHC, *Phys. Rev. D* **72**, 055001 (2005).
- [11] M. Hashimoto and K. Yamawaki, Techni-dilaton at conformal edge, *Phys. Rev. D* **83**, 015008 (2011).
- [12] T. Appelquist and Y. Bai, A light dilaton in walking gauge theories, *Phys. Rev. D* **82**, 071701 (2010).
- [13] L. Vecchi, Phenomenology of a light scalar: The dilaton, *Phys. Rev. D* **82**, 076009 (2010).
- [14] Z. Chacko and R. K. Mishra, Effective theory of a light dilaton, *Phys. Rev. D* **87**, 115006 (2013).
- [15] B. Bellazzini, C. Csaki, J. Hubisz, J. Serra, and J. Terning, A Higgslike dilaton, *Eur. Phys. J. C* **73**, 2333 (2013).
- [16] B. Bellazzini, C. Csaki, J. Hubisz, J. Serra, and J. Terning, A naturally light dilaton and a small cosmological constant, *Eur. Phys. J. C* **74**, 2790 (2014).
- [17] T. Abe, R. Kitano, Y. Konishi, K. y. Oda, J. Sato, and S. Sugiyama, Minimal dilaton model, *Phys. Rev. D* **86**, 115016 (2012).
- [18] E. Eichten, K. Lane, and A. Martin, A Higgs impostor in low-scale technicolor, [arXiv:1210.5462](https://arxiv.org/abs/1210.5462).
- [19] P. Hernandez-Leon and L. Merlo, Distinguishing a Higgs-like dilaton scenario with a complete bosonic effective field theory basis, *Phys. Rev. D* **96**, 075008 (2017).
- [20] S. Matsuzaki and K. Yamawaki, Dilaton Chiral Perturbation Theory: Determining the Mass and Decay Constant of the Technidilaton on the Lattice, *Phys. Rev. Lett.* **113**, 082002 (2014).
- [21] M. Golterman and Y. Shamir, Low-energy effective action for pions and a dilatonic meson, *Phys. Rev. D* **94**, 054502 (2016).
- [22] A. Kasai, K. i. Okumura, and H. Suzuki, A dilaton-pion mass relation, [arXiv:1609.02264](https://arxiv.org/abs/1609.02264).
- [23] M. Hansen, K. Langaebler, and F. Sannino, Extending chiral perturbation theory with an isosinglet scalar, *Phys. Rev. D* **95**, 036005 (2017).
- [24] M. Golterman and Y. Shamir, Effective pion mass term and the trace anomaly, *Phys. Rev. D* **95**, 016003 (2017).
- [25] T. Appelquist, J. Ingoldby, and M. Piai, Dilaton EFT framework for lattice data, *J. High Energy Phys.* **07** (2017) 035.
- [26] T. Appelquist, J. Ingoldby, and M. Piai, Analysis of a dilaton EFT for lattice data, *J. High Energy Phys.* **03** (2018) 039.
- [27] M. Golterman and Y. Shamir, Large-mass regime of the dilaton-pion low-energy effective theory, *Phys. Rev. D* **98**, 056025 (2018).
- [28] O. Cata and C. Muller, Chiral effective theories with a light scalar at one loop, *Nucl. Phys.* **B952**, 114938 (2020).
- [29] T. Appelquist, J. Ingoldby, and M. Piai, Dilaton potential and lattice data, *Phys. Rev. D* **101**, 075025 (2020).
- [30] O. Catà, R. J. Crewther, and L. C. Tunstall, Crawling technicolor, *Phys. Rev. D* **100**, 095007 (2019).
- [31] M. Golterman, E. T. Neil, and Y. Shamir, Application of dilaton chiral perturbation theory to $N_f = 8$, SU(3) spectral data, *Phys. Rev. D* **102**, 034515 (2020).
- [32] M. Golterman and Y. Shamir, Explorations beyond dilaton chiral perturbation theory in the eight-flavor SU(3) gauge theory, *Phys. Rev. D* **102**, 114507 (2020).
- [33] T. Appelquist *et al.* (Lattice Strong Dynamics (LSD)), Goldstone boson scattering with a light composite scalar, *Phys. Rev. D* **105**, 034505 (2022).
- [34] T. Appelquist, J. Ingoldby, and M. Piai, Nearly Conformal Composite Higgs Model, *Phys. Rev. Lett.* **126**, 191804 (2021).
- [35] T. Appelquist, J. Ingoldby, and M. Piai, Composite two-Higgs doublet model from dilaton effective field theory, *Nucl. Phys.* **B983**, 115930 (2022).
- [36] T. Appelquist, J. Ingoldby, and M. Piai, Dilaton effective field theory, *Universe* **9**, 10 (2023).
- [37] Y. Aoki *et al.* (LatKMI Collaboration), Light composite scalar in eight-flavor QCD on the lattice, *Phys. Rev. D* **89**, 111502 (2014).
- [38] T. Appelquist *et al.*, Strongly interacting dynamics and the search for new physics at the LHC, *Phys. Rev. D* **93**, 114514 (2016).
- [39] Y. Aoki *et al.* (LatKMI Collaboration), Light flavor-singlet scalars and walking signals in $N_f = 8$ QCD on the lattice, *Phys. Rev. D* **96**, 014508 (2017).
- [40] A. D. Gasbarro and G. T. Fleming, Examining the low energy dynamics of walking gauge theory, *Proc. Sci. LATTICE2016* (2017) 242 [[arXiv:1702.00480](https://arxiv.org/abs/1702.00480)].
- [41] T. Appelquist *et al.* (Lattice Strong Dynamics Collaboration), Nonperturbative investigations of SU(3) gauge theory with eight dynamical flavors, *Phys. Rev. D* **99**, 014509 (2019).
- [42] A. Hasenfratz, Emergent strongly coupled ultraviolet fixed point in four dimensions with eight Kähler-Dirac fermions, *Phys. Rev. D* **106**, 014513 (2022).
- [43] Z. Fodor, K. Holland, J. Kuti, D. Negradi, C. Schroeder, and C. H. Wong, Can the nearly conformal sextet gauge model hide the Higgs impostor?, *Phys. Lett. B* **718**, 657 (2012).
- [44] Z. Fodor, K. Holland, J. Kuti, S. Mondal, D. Negradi, and C. H. Wong, Toward the minimal realization of a light composite Higgs, *Proc. Sci. LATTICE2014* (2015) 244 [[arXiv:1502.00028](https://arxiv.org/abs/1502.00028)].

- [45] Z. Fodor, K. Holland, J. Kuti, S. Mondal, D. Negradi, and C. H. Wong, Status of a minimal composite Higgs theory, *Proc. Sci. LATTICE2015* (**2016**) 219 [arXiv:1605.08750].
- [46] Z. Fodor, K. Holland, J. Kuti, D. Negradi, and C. H. Wong, The twelve-flavor β -function and dilaton tests of the sextet scalar, *EPJ Web Conf.* **175**, 08015 (2018).
- [47] Z. Fodor, K. Holland, J. Kuti, and C. H. Wong, Tantalizing dilaton tests from a near-conformal EFT, *Proc. Sci. LATTICE2018* (**2019**) 196 [arXiv:1901.06324].
- [48] Z. Fodor, K. Holland, J. Kuti, and C. H. Wong, Dilaton EFT from p-regime to RMT in the ϵ -regime, *Proc. Sci. LATTICE2019* (**2020**) 246 [arXiv:2002.05163].
- [49] J. M. Maldacena, The large N limit of superconformal field theories and supergravity, *Int. J. Theor. Phys.* **38**, 1113 (1999); *Adv. Theor. Math. Phys.* **2**, 231 (1998).
- [50] S. S. Gubser, I. R. Klebanov, and A. M. Polyakov, Gauge theory correlators from noncritical string theory, *Phys. Lett. B* **428**, 105 (1998).
- [51] E. Witten, Anti-de Sitter space and holography, *Adv. Theor. Math. Phys.* **2**, 253 (1998).
- [52] O. Aharony, S. S. Gubser, J. M. Maldacena, H. Ooguri, and Y. Oz, Large N field theories, string theory and gravity, *Phys. Rep.* **323**, 183 (2000).
- [53] W. D. Goldberger and M. B. Wise, Modulus Stabilization with Bulk Fields, *Phys. Rev. Lett.* **83**, 4922 (1999).
- [54] O. DeWolfe, D. Z. Freedman, S. S. Gubser, and A. Karch, Modeling the fifth-dimension with scalars and gravity, *Phys. Rev. D* **62**, 046008 (2000).
- [55] W. D. Goldberger and M. B. Wise, Phenomenology of a stabilized modulus, *Phys. Lett. B* **475**, 275 (2000).
- [56] C. Csaki, M. L. Graesser, and G. D. Kribs, Radion dynamics and electroweak physics, *Phys. Rev. D* **63**, 065002 (2001).
- [57] N. Arkani-Hamed, M. Porrati, and L. Randall, Holography and phenomenology, *J. High Energy Phys.* **08** (2001) 017.
- [58] R. Rattazzi and A. Zaffaroni, Comments on the holographic picture of the Randall-Sundrum model, *J. High Energy Phys.* **04** (2001) 021.
- [59] L. Kofman, J. Martin, and M. Peloso, Exact identification of the radion and its coupling to the observable sector, *Phys. Rev. D* **70**, 085015 (2004).
- [60] D. Elander and M. Piai, A composite light scalar, electroweak symmetry breaking and the recent LHC searches, *Nucl. Phys.* **B864**, 241 (2012).
- [61] D. Kutasov, J. Lin, and A. Parnachev, Holographic walking from tachyon DBI, *Nucl. Phys.* **B863**, 361 (2012).
- [62] R. Lawrance and M. Piai, Holographic technidilaton and LHC searches, *Int. J. Mod. Phys. A* **28**, 1350081 (2013).
- [63] D. Elander and M. Piai, The decay constant of the holographic techni-dilaton and the 125 GeV boson, *Nucl. Phys.* **B867**, 779 (2013).
- [64] M. Goykhman and A. Parnachev, S-parameter, technimeasons, and phase transitions in holographic tachyon DBI models, *Phys. Rev. D* **87**, 026007 (2013).
- [65] N. Evans and K. Tuominen, Holographic modelling of a light technidilaton, *Phys. Rev. D* **87**, 086003 (2013).
- [66] E. Megias and O. Pujolas, Naturally light dilatons from nearly marginal deformations, *J. High Energy Phys.* **08** (2014) 081.
- [67] D. Elander, R. Lawrance, and M. Piai, Hyperscaling violation and electroweak symmetry breaking, *Nucl. Phys.* **B897**, 583 (2015).
- [68] D. Elander, C. Nunez, and M. Piai, A light scalar from walking solutions in gauge-string duality, *Phys. Lett. B* **686**, 64 (2010).
- [69] D. Elander and M. Piai, On the glueball spectrum of walking backgrounds from wrapped-D5 gravity duals, *Nucl. Phys.* **B871**, 164 (2013).
- [70] D. Elander, Light scalar from deformations of the Klebanov-Strassler background, *Phys. Rev. D* **91**, 126012 (2015).
- [71] D. Elander and M. Piai, Calculable mass hierarchies and a light dilaton from gravity duals, *Phys. Lett. B* **772**, 110 (2017).
- [72] D. Elander and M. Piai, Glueballs on the baryonic branch of Klebanov-Strassler: Dimensional deconstruction and a light scalar particle, *J. High Energy Phys.* **06** (2017) 003.
- [73] E. Witten, Anti-de Sitter space, thermal phase transition, and confinement in gauge theories, *Adv. Theor. Math. Phys.* **2**, 505 (1998).
- [74] T. Sakai and S. Sugimoto, Low energy hadron physics in holographic QCD, *Prog. Theor. Phys.* **113**, 843 (2005).
- [75] T. Sakai and S. Sugimoto, More on a holographic dual of QCD, *Prog. Theor. Phys.* **114**, 1083 (2005).
- [76] R. C. Brower, S. D. Mathur, and C. I. Tan, Glueball spectrum for QCD from AdS supergravity duality, *Nucl. Phys.* **B587**, 249 (2000).
- [77] C. K. Wen and H. X. Yang, QCD(4) glueball masses from AdS(6) black hole description, *Mod. Phys. Lett. A* **20**, 997 (2005).
- [78] S. Kuperstein and J. Sonnenschein, Non-critical, near extremal AdS(6) background as a holographic laboratory of four dimensional YM theory, *J. High Energy Phys.* **11** (2004) 026.
- [79] D. Elander, A. F. Faedo, C. Hoyos, D. Mateos, and M. Piai, Multiscale confining dynamics from holographic RG flows, *J. High Energy Phys.* **05** (2014) 003.
- [80] D. Elander, M. Piai, and J. Roughley, Holographic glueballs from the circle reduction of Romans supergravity, *J. High Energy Phys.* **02** (2019) 101.
- [81] M. Bianchi, M. Prisco, and W. Mueck, New results on holographic three point functions, *J. High Energy Phys.* **11** (2003) 052.
- [82] M. Berg, M. Haack, and W. Mueck, Bulk dynamics in confining gauge theories, *Nucl. Phys.* **B736**, 82 (2006).
- [83] M. Berg, M. Haack, and W. Mueck, Glueballs vs. gluino-balls: Fluctuation spectra in non-AdS/non-CFT, *Nucl. Phys.* **B789**, 1 (2008).
- [84] D. Elander, Glueball spectra of SQCD-like theories, *J. High Energy Phys.* **03** (2010) 114.
- [85] D. Elander and M. Piai, Light scalars from a compact fifth dimension, *J. High Energy Phys.* **01** (2011) 026.
- [86] D. Elander, M. Piai, and J. Roughley, Probing the holographic dilaton, *J. High Energy Phys.* **06** (2020) 177.
- [87] M. Bianchi, D. Z. Freedman, and K. Skenderis, Holographic renormalization, *Nucl. Phys.* **B631**, 159 (2002).
- [88] K. Skenderis, Lecture notes on holographic renormalization, *Classical Quantum Gravity* **19**, 5849 (2002).

- [89] I. Papadimitriou and K. Skenderis, AdS/CFT correspondence and geometry, *IRMA Lect. Math. Theor. Phys.* **8**, 73 (2005).
- [90] C. Csaki, J. Erlich, T.J. Hollowood, and J. Terning, Holographic RG and cosmology in theories with quasilo-calized gravity, *Phys. Rev. D* **63**, 065019 (2001).
- [91] D. B. Kaplan, J. W. Lee, D. T. Son, and M. A. Stephanov, Conformality lost, *Phys. Rev. D* **80**, 125005 (2009).
- [92] V. Gorbenko, S. Rychkov, and B. Zan, Walking, weak first-order transitions, and complex CFTs, *J. High Energy Phys.* **10** (2018) 108.
- [93] V. Gorbenko, S. Rychkov, and B. Zan, Walking, weak first-order transitions, and complex CFTs II. Two-dimensional Potts model at $Q > 4$, *SciPost Phys.* **5**, 050 (2018).
- [94] A. Pomarol, O. Pujolas, and L. Salas, Holographic conformal transition and light scalars, *J. High Energy Phys.* **10** (2019) 202.
- [95] J. Cruz Rojas, D. K. Hong, S. H. Im, and M. Järvinen, Holographic light dilaton at the conformal edge, *J. High Energy Phys.* **05** (2023) 204.
- [96] P. Breitenlohner and D. Z. Freedman, Stability in gauged extended supergravity, *Ann. Phys. (N.Y.)* **144**, 249 (1982).
- [97] D. Elander, M. Piai, and J. Roughley, Dilatonic states near holographic phase transitions, *Phys. Rev. D* **103**, 106018 (2021).
- [98] D. Elander, M. Piai, and J. Roughley, Light dilaton in a metastable vacuum, *Phys. Rev. D* **103**, 046009 (2021).
- [99] D. Elander, M. Piai, and J. Roughley, Coulomb branch of $N = 4$ SYM and dilatonic scions in supergravity, *Phys. Rev. D* **104**, 046003 (2021).
- [100] D. Arean, I. Iatrakis, M. Järvinen, and E. Kiritsis, V-QCD: Spectra, the dilaton and the S-parameter, *Phys. Lett. B* **720**, 219 (2013).
- [101] D. Areán, I. Iatrakis, M. Järvinen, and E. Kiritsis, The discontinuities of conformal transitions and mass spectra of V-QCD, *J. High Energy Phys.* **11** (2013) 068.
- [102] D. Z. Freedman, C. Nunez, M. Schnabl, and K. Skenderis, Fake supergravity and domain wall stability, *Phys. Rev. D* **69**, 104027 (2004).
- [103] S. J. Rey and J. T. Yee, Macroscopic strings as heavy quarks in large N gauge theory and anti-de Sitter supergravity, *Eur. Phys. J. C* **22**, 379 (2001).
- [104] J. M. Maldacena, Wilson Loops in Large N Field Theories, *Phys. Rev. Lett.* **80**, 4859 (1998).
- [105] Y. Kinar, E. Schreiber, and J. Sonnenschein, $Q\bar{Q}$ potential from strings in curved space-time: Classical results, *Nucl. Phys.* **B566**, 103 (2000).
- [106] A. Brandhuber and K. Sfetsos, Wilson loops from multicenter and rotating branes, mass gaps and phase structure in gauge theories, *Adv. Theor. Math. Phys.* **3**, 851 (1999).
- [107] S. D. Avramis, K. Sfetsos, and K. Siampos, Stability of strings dual to flux tubes between static quarks in $N = 4$ SYM, *Nucl. Phys.* **B769**, 44 (2007).
- [108] C. Nunez, M. Piai, and A. Rago, Wilson loops in string duals of walking and flavored systems, *Phys. Rev. D* **81**, 086001 (2010).
- [109] S. S. Gubser, Curvature singularities: The good, the bad, and the naked, *Adv. Theor. Math. Phys.* **4**, 679 (2000).
- [110] N. Bobev, H. Elvang, D. Z. Freedman, and S. S. Pufu, Holography for $N = 2^*$ on S^4 , *J. High Energy Phys.* **07** (2014) 001.
- [111] D. Elander, A. F. Faedo, D. Mateos, D. Pravos, and J. G. Subils, Mass spectrum of gapped, non-confining theories with multi-scale dynamics, *J. High Energy Phys.* **05** (2019) 175.
- [112] D. Elander and M. Piai, Towards top-down holographic composite Higgs: Minimal coset from maximal supergravity, *J. High Energy Phys.* **03** (2022) 049.
- [113] D. Elander, A. Fatemiabhari, and M. Piai, Toward minimal composite Higgs models from regular geometries in bottom-up holography, *Phys. Rev. D* **107**, 115021 (2023).
- [114] D. Elander, A. Fatemiabhari, and M. Piai, A note on holographic vacuum alignment (to be published).
- [115] D. Elander, A. Fatemiabhari, and M. Piai, A new bottom-up holographic composite Higgs model (to be published).
- [116] D. Elander, A. Fatemiabhari, and M. Piai, Phase transitions and light scalars in bottom-up holography—data release, Zenodo (2022), [10.5281/zenodo.7477647](https://doi.org/10.5281/zenodo.7477647).
- [117] E. Bennett, Status of reproducibility and open science in hep-lat in 2021, *Proc. Sci. LATTICE2022* (2023) 337.
- [118] A. Athenodorou, E. Bennett, J. Lenz, and E. Papadopoulou, Open science in lattice gauge theory community, *Proc. Sci. LATTICE2022* (2023) 341.